A Three-Dimensional Muscle Biomaterial Complex *In Vitro* Organoid System: An Autoinduction Bone Formation Model

Tao He

München 2020

Aus der Klinik und Poliklinik für Orthopädie, Physikalische Medizin und
Rehabilitation

Klinik der Ludwig-Maximilians-Universität München

Direktor: Prof. Dr. med. Dipl.-Ing. Volkmar Jansson

A Three-Dimensional Muscle-Biomaterial-Complex *In Vitro* Organoid System: An Autoinduction Bone Formation Model

Dissertation
zum Erwerb des Doktorgrades der Humanbiologie
an der Medizinischen Fakultät der
Ludwig-Maximilians-Universität zu München

vorgelegt von

Tao He

aus

Siping, China

2020

Mit Genehmigung der Medizinischen Fakultät der Universität München

Berichterstatter: PD Dr. med. Jörg Hausdorf

Mitberichterstatter: PD Dr. med. Thomas Holzbach
                                           Prof. Dr. med. Hans Polzer

Mitbetreuung durch den
promovierten Mitarbeiter: Dr. Roland M. Klar

Dekan: Prof. Dr. med. dent. Reinhard Hickel

Tag der mündlichen Prüfung: 21. 07. 2020

Eidesstattliche Erklärung

Ich erkläre hiermit an Eidesstatt,

dass ich die vorliegende Dissertation mit dem Titel „A Three-Dimensional Muscle Biomaterial Complex *In vitro* Organoid System: An Autoinduction Bone Formation Model" selbständig verfasst, mich außer der angegebenen keiner weiteren Hilfsmittel bedient und alle Erkenntnisse, die aus dem Schrifttum ganz oder annähernd übernommen sind als solche kenntlich gemacht und nach ihrer Herkunft unter Bezeichnung der Fundstellen einzeln nachgewiesen habe.

Ich erkläre des Weiteren, dass die hier vorgelegte Dissertation nicht in gleicher oder in ähnlicher Form bei einer anderen Stelle zur Erlangung eines akademischen Grades eingereicht wurde

München, am 06.08.2020

_____

Tao He

Zusammenfassung

Die Übertragung von Tierversuchen in die klinische Umgebung bleibt problematisch, da das Tiersystem die menschliche *In-vivo*-Umgebung nicht angemessen repliziert. Als gute Alternative haben sich Bioreaktoren herauskristallisiert, die *in vivo* Prozesse und Organe des Menschen *in vitro* reproduzieren können. Das Ziel dieser Studie war es, ein neues Organoides *In-vitro*-Kulturmodell zu entwerfen, das lange Kulturperioden *in vitro* überstehen kann, und die knocheninduktiven Eigenschaften dieses Systems unter Verwendung von aus Korallen stammenden makroporösen Vorrichtungen zu testen, die spontan die Knochenbildung induzieren. Das langfristige Ziel dieser Experimente und anderer Studien ist die Entwicklung eines neuartigen Bioreaktorsystems, mit dem menschlicher Knochen entweder für experimentelle Studien, direkte klinische Transplantationen oder die direkte Regeneration von verlorenem osteogenem Gewebe bei Patienten synthetisch gezüchtet werden kann. Für den ersten Teil der Studie, der sich mit dem Überlebensaspekt von dem Organoiden Model befasste, wurden dreidimensional gedruckte β-Tricalciumphosphat / Hydroxyapatit (β-TCP / HA) -Anlagen entweder in eine Hülle aus Rattenmuskelgewebe eingewickelt oder zuerst heterotop in eine Muskelgewebehülle implantiert, dann herausgeschnitten und *in vitro* für bis zu 30 Tage kultiviert. Die Resultate im Muskelbeutel Organoid Modell zeigten angiogene und begrenzte prä-osteogene Genexpressionstendenzen mit konsistenter Hochregulation von *TGF-ß₁*, *COL4A1*, *VEGF-A*, *RUNX-2* bzw. *BMP-2*. Histologisch wurde ein Abbau des Muskelgewebes mit Fibrinfreisetzung beobachtet, die von den Anlagen absorbiert wurde, die möglicherweise als Unterstützung für die Neubildung von Gewebe fungieren, wobei postuliert wurde, dass das Muskelgewebe als kataboles Reservoir fungiert, das *in vitro*

wiederaufbereitet wird, um die Entwicklung von neuem anabolem Bindegewebe zu unterstützen und auch die osteogene Differenzierung von Vorläuferstammzellen in dem biokeramischen Gerüst. Nachdem das erste Ziel erreicht worden war und ein relevantes organoides Modell entwickelt worden war, wurde eine makroporöse biomimetische Anlage aus Korallen, das sich *in vivo* als wirksam erwiesen hat, um spontan die Knochenbildung zu induzieren, in das Beutelmodell eingeführt. Auch wurde die Kultivierungszeitspanne auf bis zu 60 Tage verlängert. *VEGF-A* und *OCN* waren beide hochreguliert in der Transkriptions- oder Translationsebene, wobei das konstant hochregulierte *COL4A1*-, *RUNX-2*-, *BMP-2*- und *BMP-6*-Expressionsmuster das Potenzial für Angiogenese und Osteogenese innerhalb dieses Systems implizierte. Im Anschluss an diese Entdeckungen zeigten die Ergebnisse mit dem osteogenen Medium auch, dass in diesem organoiden Muskelsystem das Medium die Osteogenese nicht unterstützt, wie allgemein angenommen wird, sondern nur die hypertrophe Verschlechterung des Gewebes mit zunehmender Kulturzeit fördert. Dies macht das osteogene Medium für *In-vitro*-Tests ungeeignet, da es zu irreführenden Ergebnissen führt, die keiner echten osteogenen Körperreaktion entsprechen. Diese Ergebnisse zeigen daher, dass das auf einem Skelettmuskelbeutel basierende Biomaterial-Kultursystem das Überleben des Gewebes über einen längeren Kulturzeitraum unterstützen kann und ein neues Organoid-Gewebemodell darstellt, das mit weiteren Anpassungen in zukünftigen Studien reines Knochengewebe erzeugen könnte.

Summary

The translation from animal research into the clinical environment remains problematic, as animal system do not adequately replicate the human *in vivo* environment. Bioreactors have emerged as good alternative that can reproduce the human *in vivo* processes and organs at an *in vitro* level. As such the aim of the present study was to design a new organoid *in vitro* culture model that could survive long culture periods *in vitro* and to test the bone inductive qualities of this system using coral derived macroporous devices that spontaneously induce bone formation. The long-term goal of these experiments and other studies is to develop a novel bioreactor system that can synthetically grow human bone for either experimental studies, direct clinical transplantations or directly regenerate lost osteogenic tissue on patients. For the first part of the study, dealing with the organoid survival aspect, three-dimensional printed β-tri-calcium phosphate/hydroxyapatite (β-TCP/HA) devices were either wrapped in a sheet of rat muscle tissue or first implanted in a heterotopic muscle pouch that was then excised and cultured *in vitro* for up to 30 days. Devices wrapped in muscle tissue necrosed by day 15. Contrarily, devices in muscle pouches showed angiogenic and limited pre-osteogenic gene expression tendencies with consistent *TGF-β₁*, *COL4A1*, *VEGF-A*, *RUNX-2*, and *BMP-2* upregulation, respectively. Histologically, muscle tissue degradation with fibrin release was seen being absorbed by devices acting possibly as a support for new tissue formation where it is postulated that the muscle tissue acts as catabolic reservoir that *in vitro* is repurposed to supported new anabolic connective tissue development and ingrowth into the bioceramic scaffold with progenitor stem cell osteogenic differentiation. With the first goal achieved and possessing a relevant organoid model, a coral-derived macroporous biomimetic device, proven to be effective *in vivo* to

spontaneously induce bone formation, was then introduced to the pouch model, replacing the β-TCP/HA device with *in vitro* culture periods being extended up to 60 days. *VEGF-A* and *OCN* were both upregulated either at the transcriptional or translational level, with the constant upregulated *COL4A1*, *RUNX-2*, *BMP-2* and *BMP-6* expression pattern, implying the potential for angiogenesis and osteogenesis within this system. Subsequent to these discoveries the results of the "osteogenic" medium also showed that within this muscle pouch organoid system, this medium type does not, as globally believed, support osteogenesis, but rather accelerates the hypertrophic deterioration of the tissue as culture time increases. This makes osteogenic medium unsuitable for *in vitro* testing as it creates misleading results that do not correspond with a true osteogenic environmental reaction. These results therefore demonstrate that the skeletal muscle pouch-based biomaterial culturing system can support tissue survival over an extended long culture period and represents a novel organoid tissue model that with further adjustments could generate pure bone tissue in the future studies.

Publications

He, T., Hausdorf, J., Chevalier, Y., & Klar, R.M. (2020).

Trauma induced tissue survival in vitro with a muscle-biomaterial based osteogenic organoid system: a proof of concept study.

BMC Biotechnol, 31;20(1):8. doi: 10.1186/s12896-020-0602-y.

He, T., Huang, Y., Chak, J. C., & Klar, R. M. (2018).

Recommendations for improving accuracy of gene expression data in bone and cartilage tissue engineering.

Sci Rep, 8(1), 14874. doi:10.1038/s41598-018-33242-z

Teng, A., Liu, F., Zhou, D., **He, T.**, Chevalier, Y., & Klar, R. M. (2018).

Effectiveness of 3-dimensional shoulder ultrasound in the diagnosis of rotator cuff tears: A meta-analysis.

Medicine (Baltimore), 97(37), e12405. doi:10.1097/MD.0000000000012405

He, T., Cao, C., Xu, Z., Li, G., Cao, H., Liu, X., Zhang, C., & Dong, Y. (2017).

A comparison of micro-CT and histomorphometry for evaluation of osseointegration of PEO-coated titanium implants in a rat model.

Sci Rep, 7(1), 16270. doi:10.1038/s41598-017-16465-4

Presentations at Meetings/Conferences

He T., Hausdorf J., Hasselt S., Seitz D., Chevalier Y., Mueller P.E., Jansson V., Klar R.M. Metabolic tissue vasculo-metamorphosis *in vitro*: a bone induction model.

 XI. Münchener Symposium für experimentelle Orthopädie, Unfallchirurgie und muskuloskelettale Forschung, Munich, 2019. (Oral)

This work is dedicated to my family and friends who made it possible for me

to spend days and weeks to compose this thesis without feeling guilty

about the time I spent away from them.

Acknowledgements

Table of Contents

Abbreviations

kg	kilogram
mg	milligram
μg	microgram
pg	picogram
ml	milliliters
μl	microliters
mm	millimeters
μm	micrometers
mM	millimolar
μM	micromolar
nM	nanomolar
IU	international unit
ACAN	aggrecan
ADSCs	adipose-derived stem cells
ALP	alkaline phosphatase
AP-1	activator protein 1
ATF4	activating transcription factor 4
BMP	bone morphogenetic protein
BMSCs	bone marrow stem cells
β-TCP/HA	β-tricalcium phosphate/hydroxyapatite
HA/CC	hydroxyapatite/calcium carbonate
cDNA	complementary DNA
COL4A1	collagen type IV alpha 1
CNRQs	calibrated normalized relative quantities
DMEM	Dulbecco's modified Eagle medium
DMEM-hg	Dulbecco's modified Eagle medium–high glucose
ECM	extracellular matrix
FGF	fibroblast growth factor

HA	hydroxyapatite
HE	hematoxylin and eosin
IGF-1	Insulin like growth factor-1
IHH	Indian hedgehog homolog
IOD	integrated optical density
mRNA	messenger ribose nucleic acid
MPCs	mesenchymal progenitor cells
MSCs	mesenchymal stem cells
MOD	mean optical density
OCN	osteocalcin
OP-1	osteogenic protein-1
OSF-1	osteoblast-stimulating factor-1
PA	positive area
PCR	polymerase chain reactions
POLR2E	RNA polymerase II subunit E
qRT-PCR	quantitative real-time polymerase chain reactions
RNA	ribose nucleic acid
ROI	region of interest
RPLP0	ribosomal protein large P0
RUNX-2	Runt-related transcription factor 2
SDHA	succinate dehydrogenase complex subunit A
3D	three dimensional
TBP	TATA binding protein
TGF	transforming growth factor
VEGF-A	vascular endothelial growth factor A
Wnts	wingless-related integration site proteins

List of Tables

List of Tables

List of Figures

formation at the interface of the muscle and device (**C**, **D**; pink arrows). Movat pentachrome staining was utilized to assess for collagen associated with chondrogenesis and osteogenesis, elastic fibers, muscle and connective tissue. Bars: **A, B, D, E, F** and **H** = 100μm; **C** and **G** = 200 μm.

CHAPTER 1
INTRODUCTION WITH LITERATURE REVIEW

The bone tissue engineering challenge

The effective translation from *in vitro* to *in vivo* and *in vivo* to clinical practice remains a major challenge for tissue regenerative sciences (Anderer and Libera, 2002; Reichert et al., 2009; Amini et al., 2012; Denayer et al., 2014). Whilst experimental *in vitro* and *in vivo* investigations continue to contribute greatly to deciphering specific criteria in biological sciences, the translation from a functional model to the clinical setting takes an exuberant amount of time and consumes vast resources (Collier, 2009). This is one of the reasons why bone tissue induction models are not yet used and the autogenous bone graft (Havers and Geuder, 1692; Ollier, 1867; Senn, 1889; Galindo-Moreno et al., 2008; Nkenke and Stelzle, 2009; Atef et al., 2019) remains the golden standard for bone regeneration clinically. The following sections provide an overview of the challenges faced in the prospect to regenerate bone *in vivo* setting where alternative and yet unexplored research holds perhaps the solutions to solving the enigma for how to engineer bone tissue, clinically.

1.1 Induction of bone formation

The induction of bone formation defines the process of bone formation that is stimulated in sites of the body not normally associated with the super-organ bone. These sites can, but are not limited to, muscle tissue, organs including adipose deposits. Bone tissue regeneration and its subsequent engineering through science derives from a rich past (Urist, 1965; Reddi, 2000; Ripamonti, 2006) and present (Klar, 2018). In order to understand the principle of bone induction, the foundations that have led to its development are key as all developed principles, from experimental theories, have a unique role and to ignore this history is to repeat the mistakes of the past.

It all started from the founding principle discovered by Senn (1889) nearly two centuries ago. Without the research done by Senn (1889) the ideas and principles that shape the modern concept of bone formation by inducing bone formation may never have emerged. Senn (1889) performed a series of implantations into skull defects of canines using decalcified antiseptic bone cuts and was the first to discover that decalcified bone possessed new bone formation potential, that would only much later under Levander, 1945 become known as induction. Subsequent to the findings that decalcified bone cuts could undergo new osteogenesis in bony defect sites, Senn (1889) also by accident discovered that the surrounding of the implant was often showing new embryonic-like tissue formation thereby indirectly suggesting the process of osteogenesis within these bone "devices" was a recapitulation of embryonic processes that normally only occur during fetal development (Levander, 1938).

Whilst it still remains debatable today whether the implantation of decalcified bone material implanted into a bone defect site by Senn 1889 can truly be considered as bone induction, follow up experiments in uroepithelial tissue by Huggins, 1931 indeed proved that bone formation could be "induced" within non-bony extra-skeletal sites. Subsequent studies utilizing partially extracted ethanol-treated bone matrices and then implanted in heterotopic sites of rats could also induced new bone formation (Levander, 1938; Willestaedt et al., 1950) supporting further Senn 1889 observations regarding the recapitulatory events of embryogenesis. Concomitantly, by 1968 the theory of some unknown as yet to be classified "substance" that resided within bone was also postulated (Friedenstein, 1968) which was previously theorized to be "osteogenin" (Lacroix, 1945) a molecule or particle that possesses the capability to induce new bone formation.

However, it would be the pioneering research by Urist, 1965, who identified key criteria form the investigations and reports from Senn, Huggins, Levander, Lacroix, which then through his own analyses would culminate in the groundbreaking the foundations and principles that would become known as the autoinduction principle of bone formation (Urist, 1965; Urist et al., 1967). Additionally, he would go on to re-name Lacroix 1945 "osteogenin" molecule to "bone morphogenetic protein (BMP)" which Urist hypothesized was a type of compound present within the bone matrix that modulated or stimulated the reaction toward new bone formation or more appropriately "bone morphogenesis". The subsequent experiments in other animals' models would lead to the isolation of a protein family (Wang et al., 1988; Wozney et al., 1988) specifically denoted as "BMPs" (Urist et al., 1967; Urist and Strates, 1971).

Once BMPs had been successfully extracted from the extracellular matrix of bone (Reddi and Huggins, 1972; Sampath and Reddi, 1981; Reddi, 1994) the bone induction principle, postulated by Urist and Strates 1971, was eventually defined after the systematic works of Sampath and Reddi, 1981. Critical to the bone induction principle was that only when an insoluble matrix carrier and soluble molecular signals in the form of morphogens were combined would it be possible to induce new bone formation *in vivo* (Sampath and Reddi, 1981). This basis is still the foundation on which most tissue inductive models function where it has to be however noted that the principle does not apply to all scenarios especially those of the disease state of ectopic bone formation (Gonda et al., 2000; Lin et al., 2010; Wang et al., 2014; Katagiri et al., 2015) and specifically the spontaneous bone formation potential of naturally derived biomaterials such as coral derived macroporous biomimetic matrices (Ripamonti, 1990; 1991; Klar et al., 2014; Ripamonti et al., 2016).

1.2 Biomaterials

A wide range of biomimetic biomaterials have been tested in bone tissue engineering and bone regeneration, including bioactive metal, ceramics, natural and synthetic polymers, and glasses. (Ripamonti, 1991; Livingston et al., 2002; Fujimura et al., 2003; Mauney et al., 2004; Meinel et al., 2004; Nazarov et al., 2004; Kim et al., 2005; Mauney et al., 2005; Moreira-Gonzalez et al., 2005; Sul et al., 2005; Klar et al., 2013; Ye et al., 2016; He et al., 2017; Yang et al., 2017) Among them, calcium carbonate and hydroxyapatite (HA), owing to their similar chemical composition and biomechanical nature as bone tissue, are regarded amid the most promising bone graft substitute. (White et al., 1975; Daculsi et al., 1989; Ripamonti, 1990; Lu et al., 1998; Boyde et al., 1999; Flautre et al., 1999; Kon et al., 2000; Dong et al., 2001; Dong et al., 2002; Livingston et al., 2003; Gauthier et al., 2005; Mastrogiacomo et al., 2006; Cosar et al., 2008; Boos et al., 2011; Klar et al., 2013; Kakar et al., 2017) Apart from chemical composition, the stereo configuration is another critical characteristic for the efficient bone formation and ingrowth into biomaterials, including the ratio of porosity, pore size, pore shape, and the pattern and size of pore interconnection pathway. (Gauthier et al., 1998; Lu et al., 1999; Chang et al., 2000; De Oliveira et al., 2003; Karageorgiou and Kaplan, 2005; Mastrogiacomo et al., 2006) Macropores have been reported with increasing evidence to support a more comprehensive and superior bone tissue ingrowth into biomaterials *in vivo*, whereas microporous biomaterial constraints its capacity of osteoinduction and osteoconduction. (Gauthier et al., 1998; Boyde et al., 1999; Chang et al., 2000) One of the key parameters that facilitates osteoconduction in macroporous biomaterials is the pattern of pore interconnection pathway (Mastrogiacomo et al., 2006). When the size of the interconnection pathway is reduced to a certain extent, the bone tissue ingrowth will be considerably limited due to the restraint potential for larger

vessel penetration into biomaterials, ultimately restricting the size of bone graft substitute for the treatment of critical size bone defect.

1.3 The Molecular conundrum in bone tissue engineering

Expanding molecules are added into the complex molecular network as morphogens (Urist and Strates, 1971; Joyce et al., 1990; Rosen et al., 1994; Reddi, 1998; Pang et al., 2004; Mayer et al., 2005; Lin et al., 2006; Simic et al., 2006; Klar et al., 2014), signaling molecules (Itoh et al., 2001; Hsu and Huang, 2013; Yang et al., 2015; Xu et al., 2018; Morgoulis et al., 2019), transcription factors and co-regulators (Dudek et al., 2010; Javed et al., 2010; Martinez-Sanchez et al., 2012; Steck et al., 2012; Schipani et al., 2013; Dey et al., 2014; Trzeciak and Czarny-Ratajczak, 2014; Lewis et al., 2016; Komori, 2017; Lefebvre, 2019), altogether synergistically regulating the induction of bone formation process. The physiological differential process comprises mainly four phases: cell proliferation and lineage commitment, osteoprogenitor proliferation and differentiation, synthesis of extracellular matrix (ECM) and programmed osteoprogenitor apoptosis, and maturation of osteocyte with mineralization (**Figure 1**) (Javed et al., 2010). Different regulators are expressed in a rigorous spatial and temporal dependent manner at both transcriptional and translational levels. The key transcription factors include, but are not limited to, *Runt-related transcription factor 2* (*RUNX-2*), *Osterix*, *activating transcription factor 4 (ATF4), activator protein 1 (AP-1), and osteoblast-stimulating factor-1(OSF-1)*, involved in different phases of the osteogenic differentiation. At the translational level, BMPs (BMP-2, 4, 6, 7), transforming growth factor (TGF)-β isoforms (TGF-β_1, -β_2, -β_3), insulin like growth factor-1 (IGF-1), wingless-related integration site proteins (Wnts), β-

catenin, Indian hedgehog homolog (IHH), fibroblast growth factor-2 (FGF-2) and FGF-18

play integral roles in mediating mesenchymal stem cells (MSCs) differentiating into

osteocyte.

Mesenchymal Stem Cell		Osteoprogenitor		Pre-Osteoblast		Osteoblast		Osteocyte	
Self Renewal		**Proliferation & Commitment**		**Proliferation & Differentiation**		**Mineralization & Apoptosis**		**Mineralization**	
Sox2 Msx1, 2 Bapx1	Twist1 TLE CHIP	Runx2 Osterix Msx1, 2 C/EBPβ,δ Satb2	Twist1 TLE Hoxa2 Shn3 CHIP	Runx2 Osterix Nfatc1 ATF4 Satb2 AP-1	Twist1 Stat1 Shn3 WWP1	Runx2 Osterix Dlx3, 5 ATF4 C/EBPβ,δ AP-1	Stat1 Shn3 WWP1	Runx2 Osterix OSF-1	?
FGF18 GH FGFR2		BMP2 PTH Ihh GC/Dex Wnt/β-catenin	Notch TGFβ	BMP2, 6 IGF1 Wnts Ihh FGF2, 18	Notch TGFβ BMP3 Vit-D3	BMP2, 6 Wnts Ihh Vit-D3	Smad3 TGFβ BMP3 GC/Dex PTH	FGF23 BMP2	Sclerostin GC
Oct4 c-Myc Nanog CD15		SDF1 ALCAM CD 44, 63, 105 BMP/TGFβ Histone		Alk. Phosp Collagen Osteopontin BMP/TGFβ Histone Integrins		Collagen Osteopontin BSP Osteonectin Ostocalcin MMPs		E11/gp38 Phex DMP1 Ostocalcin MEPE Sclerostin	

Figure 1. Diagrammatical illustration of the developmental progression of osteoblast lineage and the list of correspondent secretory and phenotypic markers. The first row demonstrates the chronological stages of the osteoblast lineage from pluripotent stem cells to terminally differentiated osteocyte accompanied with characteristic description. The critical transcription factors involved in regulating osteoblast differentiation are listed in the second row, with inhibitors indicated in red. The third row summarizes the paracrine/autocrine secretory mediators controlling osteoblast development. Key phenotypic genes expressed in the process of osteogenic differentiation are indicated in the last row. (With permission by Javed et al. 2010)

In additional to osteoblast differentiation, angiogenesis and/or vasculogenesis shares the

same, if not even more important, role in the formation of bone tissue in a large scale, as

the permeability of soluble blocks into tissue is restricted within 2 mm where no vascular

perfusion is present, preventing the necessary nutrient support and molecular regulation for

an effective and efficient bone formation. RUNX-2, collagen type IV alpha 1 (COL4A1)

and vascular endothelial growth factor A (VEGF-A) are known as the key proteins involved in the process of angiogenesis and vasculogenesis. (Trueta, 1963; Feder et al., 1983; Ingber and Folkman, 1989; Flamme and Risau, 1992; Flamme et al., 1993; Vernon et al., 1995; Risau, 1997; Vittet et al., 1997; Arthur et al., 1998; Wartenberg et al., 1998; Goumans et al., 1999; Zhu et al., 2000; Vailhé et al., 2001; Mayer et al., 2005; Kneser et al., 2006; Polykandriotis et al., 2007; Beier et al., 2010; Amini et al., 2012; Gu et al., 2013; Bhatt and Atkins, 2014; Filipowska et al., 2017; Sharma et al., 2019)

Collectively, the exquisite interplay of a complex transcriptional and translational regulators network contributes to the true bone formation by induction, with the presence of both osteogenesis and angio-/vasculogenesis.

1.4 The animal translation enigma

The first of the bone inductive BMPs isolated and tested for its osteogenesis potential was the recombinant human BMP-2 (rhBMP-2). In a time study, recombinant human BMP-2 was able to increase cellular invasion and induced chondrogenesis within the demineralized bone matrices within just 5 days (Wang et al., 1990). Within 7 days the cartilage was beginning to be ossify and after just 21 days the bone matrix had been formed. It was therefore postulated that BMP-2 was one of the critical molecules crucial for initiating bone formation, within the insoluble substratum. Afterwards, other BMPs were assessed for their part in inducing bone formation. Specifically, BMP-4 was found to only induce bone formation at high concentration (Hammonds et al., 1991), with the BMP-5 inducing bone at a retarded level, irrelevant of application dose (Cox et al., 1991; D'alessandro, 1991).

Subsequently BMP-6, osteogenic protein-1 (OP-1/BMP-7) and BMP-9 all were discovered to induce bone formation similar to that of BMP-2 (Riley et al., 1996).

The substantial induction of bone formation in pre-clinical animal studies prematurely convinced basic scientists and skeletal reconstructioneers that an application of a single dose of a recombinant human bone morphogenetic protein would induce tissue morphogenesis, in a clinical environment (Friedlaender et al., 2001; Govender et al., 2002). However, this theoretical potential has so far not been successfully translated to clinical context. Clinical trials of craniofacial orthopaedic applications such as mandibular reconstruction have indicated that supra-physiological doses of a single recombinant human BMPs/OPs (hBMPs/OPs) are needed to often induce clinically unacceptable induction of bone, which still falls short of autogenous bone grafts (Ripamonti, 2006; Garrison et al., 2007; Mussano et al., 2007; Ripamonti et al., 2007; Ripamonti et al., 2009).

It is well known by now that *in vitro* to *in vivo* testing and subsequently *in vivo* to human trials do not properly replicate treatments clinically (Denayer et al., 2014). Criteria affecting often results from turning out positive are those of methodological design and sample size variations which are often overlooked when interpreting into the clinical aspect. In their review Denayer et al. (2014) adequately listed several factors that affect the translation from animal models into humans. Alternative criteria such as maturity of animals, differences between bones and size variations between animal models all contribute towards the translation enigma (Evans and Stoddart, 2016). Alternatively, it has to be considered that present bone induction procedures are utilizing allo-/xenografting principles that have been shown to not function *in vivo* (Ladd and Pliam, 1999; Keating and McQueen, 2001; Betz,

2002; Linovitz and Peppers, 2002; Klar, 2018), but are replicated in the form of biomaterials, utilizing autogenous bone grafting principles.

Subsequently, most studies overlook the difference between animal and human genes that, whilst structurally similar, have different expression patterns or function. Often it is assumed that animal models, in particular for inductive bone studies, are genetically compatible to each other since osteogenesis appears to be similar between all experimentally utilized animal models compared to humans. Whilst there are homologous trends in the gene structure of various animal models, with that of the human including functionality *in vivo*, a fact often left out is that in most cases subtle variations in gene structure can produce considerable difference between species.

These criteria including many others too numerous to all compile here have forced tissue engineers to consider alternative modes of research models that negate animal models completely and instead focus on using *in vitro* based systems that replicate in their totality the complexity of the human organs.

1.3 Bioreactors

Bioreactor platforms, simulating certain tissue types, have shown great capabilities at replicating certain *in vivo* environments (Martin et al., 2004; Plunkett and O'Brien, 2011). However, bioreactors remain problematic for use in forming a super-organ like bone, as there are various biochemical, cellular and mechanical requirements that need to be met to form this tissue type either ectopically or orthotopically (Urist and Strates, 1971; White et al., 1975; Sampath and Reddi, 1981; Ripamonti, 1990; Reddi, 2000; Martin et al., 2004;

Mastrogiacomo et al., 2006; Ripamonti, 2006; Plunkett and O'Brien, 2011; Klar et al., 2013; Alexander et al., 2014; Klar et al., 2014; Ripamonti et al., 2016; Costa et al., 2017; Ho et al., 2017) In brief, a proper bioreactor should be comprised of multipotent stem cells or progenitor cells located within a bone tissue ECM simulating scaffold, with tunable autocrine or paracrine biological factors regulating the system toward osteogenic morphogenesis, where a biomimetic perfusion and mechanical stimuli should also be included (**Figure 2**). Furthermore, vascularization and/or angiogenesis are essential components that help the tissue survive and grow in a size with diameter more than 2mm (Trueta, 1963; Feder et al., 1983; Flamme et al., 1993; Nakagawa et al., 1993; Risau, 1997; Vailhé et al., 2001; Filipowska et al., 2017; Sharma et al., 2019).
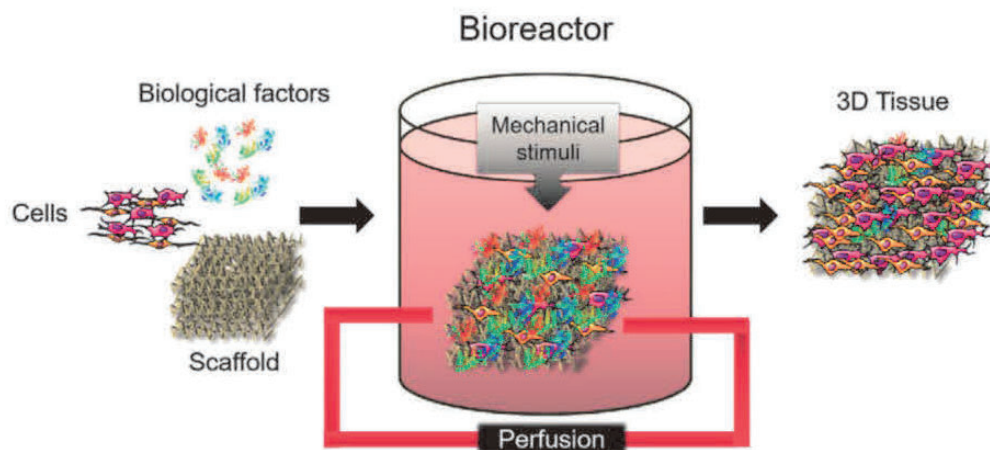
Figure 2. Schematic bioreactor for bone tissue engineering *in vitro*. (With permission by Costa et al. 2017)

Most bioreactor platforms utilize stem cells, such as bone marrow stem cells (BMSCs), MSCs and adipose-derived stem cells (ADSCs) or mesenchymal progenitor cells (MPC) on a specific biomaterial to produce a specific single cell derived tissue type, which have showed the up-regulation of different sets of osteogenic differentiation related phenotypic

markers *in vitro* and some promising evidence showing the capacity of osteo-induction and/or osteo-conduction *in vivo.* (Sottile et al., 2003; zur Nieden et al., 2003; Bonab et al., 2006; Kubo et al., 2009; Mendez-Ferrer et al., 2010; Yablonka-Reuveni, 2011; Amini et al., 2012; Bhumiratana et al., 2016; Nguyen et al., 2016; Mitra et al., 2017; De La Vega et al., 2018) However, they are still inadequate for the real bone tissue morphogenesis *in vitro* as various steps are required that together culminate in the formation of this tissue (Gilbert, 2000). Additionally, cells cultured *in vitro* not only lose their homeostatic state through the loss of essential amino acids, that growth medium can hardly supply in a controlled and released state as *in vivo* tissue breakdown would (Nelson and Cox, 2005), but also need to develop a viable ECM environment first before they can thrive and grow (Leighton et al., 1968; Blair et al., 2017). Hence, *in vivo* tissue based bone inductive studies remain to date the best models to study the effect of biomaterial behavior *in vivo*. As such, a tissue based bioreactor platform (Sakakura et al., 1989; Roach, 1990; Bhumiratana et al., 2016) could be superior to that of a stem cell based system as tissues poses various biochemical building blocks and adult stem cell niches together with pre-established cell growth promoting environments that theoretically could provide a superior culturing milieu. However, the use of bone directly as a biomaterial growth environment *in vitro* is highly problematic, as culture medium cannot adequately diffuse across a hard tissue barrier (Sakakura et al., 1989).

CHAPTER 2
RESEARCH AIMS AND OBJECTIVES

2.1 Research Aims

The present study aimed at investigating (1) the feasibility and (2) the bone induction potential of a new skeletal muscle-based biomaterial *in vitro* organoid bioreactor system utilizing rat.

2.2 Research objectives

The first objective dealt with developing a tissue-based biomaterial *in vitro* tissue model that reproduces a heterotopic inductive bone formation environment with the potential to survive long culture periods *in vitro* and showing possible signs of vasculo-/angiogenic morphogenesis, crucial for *de novo* bone formation (Trueta, 1963; Nakagawa et al., 1993). The two models tested were:

(A) A biomaterial wrapped in abdominal muscle tissue;

(B) A biomaterial placed in a pouch similar to heterotopic *in vivo* implantation models situated within the abdominal muscle tissue.

The secondary objective was then to utilize the best model from the first objective, that showed the best reactivity and survivability, to assay bone inductive processes utilizing a known and spontaneously inducing bone formation biomaterial, i.e. 7% hydroxyapatite/calcium carbonate (7% HA/CC; Ripamonti, 1990; 1991; Klar et al., 2013; Klar et al., 2014).

CHAPTER 3

MATERIALS AND METHODS

3.1 Proof-of-concept: *In vitro* tissue-biomaterial organoid model

3.1.1 Three dimensional (3D) printed β-tricalcium phosphate/hydroxyapatite (β-TCP/HA) devices

Eighteen devices were provided by BioMed Center Innovation gGmbH (Bayreuth, Germany), by Mr. Daniel Seitz. The 3D-printed β-TCP/HA bioceramic devices (**Figure 3 A**) were manufactured using a mixture of tri-calcium phosphate and hydroxyapatite powders (Merck, Kenilworth, NJ, USA)) at a ratio of 40%:60%, respectively. The mixture had previously been spray-nozzle granulated from a water-based slurry with addition of organic dispersing and binding agents using a custom spray-dryer (Trema, Kemnath) and cut off at 100 µm using a classing sieve (Retsch, Haan, Germany). The lower fraction of granulate was coated with organic adhesion-improving agents by means of fluidized bed coating; the final printing powder had size distribution values of d10 = 34.87 µm, d50 = 61.86 µm and d90 = 93.33 µm. After mixing the powder with a combination of organic additives (trade secret), the scaffolds were then printed out in a Z310 3D-Printer (3D Systems, Rock Hill, USA) using the standard colorless ink provided with the printer. After de-powdering, the scaffolds were sintered at 1250°C, producing a solid, organic-free, porous bioceramic device with macroscopic pore channels (670.52 +/- 97.60 µm) resulting from printing design and smaller internal pores (80.95 +/- 23.38 µm) as described above. The devices were then allowed to cool, after which they were cleaned using deionized water, packed and sterilized by vacuum pulse autoclaving.

3.1.2 Skeletal-muscle-based biomaterial culturing models

Four *Rattus norvegicus* Fischer 344/DuCrl adult male rats (Charles River, Sulzbach,

Germany), were utilized in the pilot study, and equally split between the two tissue models. Animals were euthanized with an overdose of isoflurane (Abbot, Chicago, USA). This was done in accordance to the rules and regulations of the Animal Protection Laboratory Animal Regulations (2013), European Directive 2010/63/EU and approved by the Animal ethics research committee (AESC) of the Ludwig Maximillian's University of Munich (LMU), Bavaria, Germany Tierschutzgesetz §1/§4/§17 (https://www.gesetze-im-internet.de/tierschg/TierSchG.pdf) with respect to animal usage for pure tissue or organ harvest only.
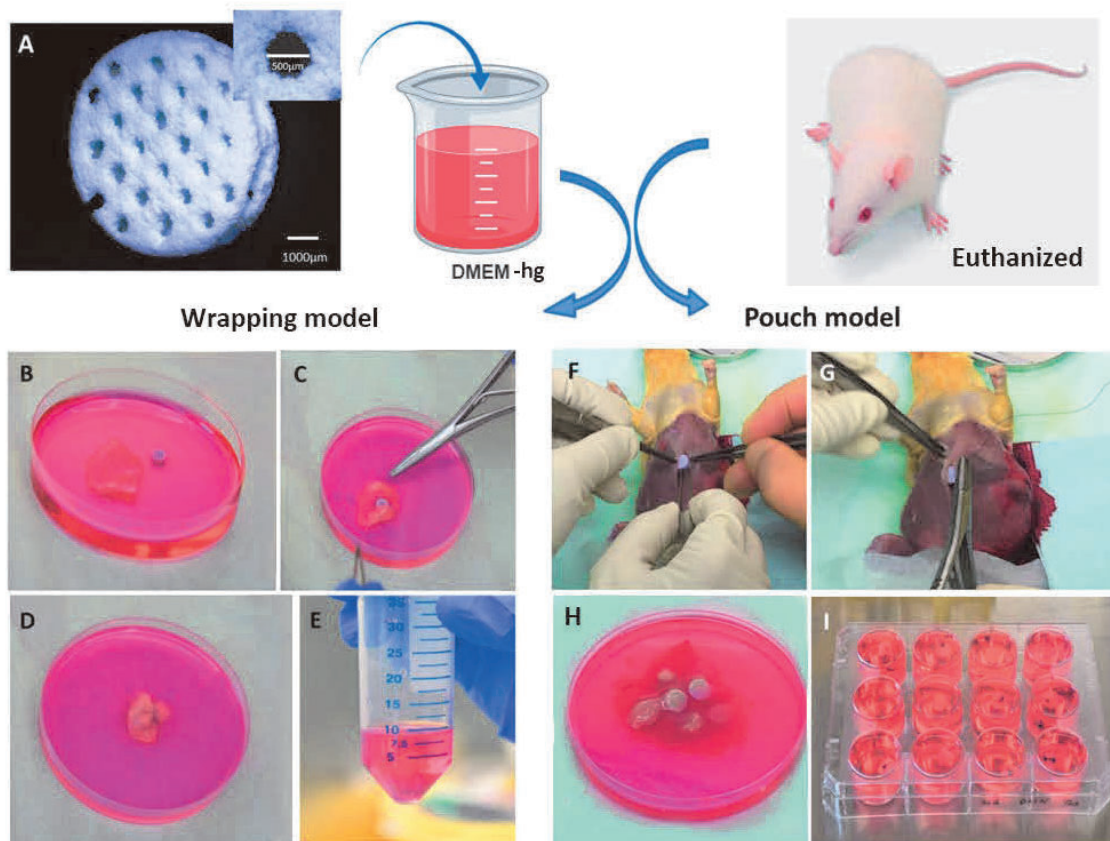
Figure 3. In vitro wrapping and heterotopic implanted bioceramic pouch model methodology (**A-I**). The three-dimensional printed macro-porous β-tricalcium phosphate/hydroxyapatite (β-TCP/HA) bioceramic devices (**A**), for the wrapping or pouch models, were placed in growth medium (DMEM), prior to either wrapping them in rat skeletal muscle tissue (**B-E**), or implanting them first in heterotopic extra-skeletal muscle sites (**F-I**) of euthanized rats, after which the implant site with devices was harvested, devices embedded in the muscle tissue excised, and subsequently placed in growth medium to be cultured for 5, 15 and 30 days in vitro.

Two skeletal muscle tissue biomaterial-based models were designed and tested:

1) Tissue wrapping model

For the tissue wrapping model, n=9 β-TCP/HA devices, were first immersed in normal growth medium composed of Dulbecco's modified Eagle medium-high glucose (DMEM-hg, Biochrom GmbH, Berlin, Germany), 40 IU/mL penicillin (Biochrom GmbH) and 40 IU/mL streptomycin (Biochrom GmbH) .

Two F-344 adult male rats (Charles River) were euthanized under sterile conditions, the abdominal skeletal muscle tissue harvested, placed in normal DMEM-hg after which 3D printed β-TCP/HA devices were wrapped in the sheets of muscle tissue (**Figure 3 B-E**). Nine β-TCP/HA devices were then wrapped with a skeletal muscle sheet, and divided into 3 culturing periods set at 5, 15 and 30 days. Each culturing period contained 3 tissue bags. Muscle tissue without β-TCP/HA devices was cultured in parallel to tissue bags and acted as controls. Medium was changed every 2 days. Fresh muscle tissue was used in the normalization of quantitative real-time polymerase chain reactions (qRT-PCR).

2) Tissue pouch model

Nine β-TCP/HA devices were prepared by placing them in normal growth medium as explained in the section of the tissue wrapping model. Rats were then euthanized under sterile conditions, β-TCP/HA devices were immediately implanted in intramuscular pouches created by sharp and blunt dissection (**Figure 3 F-I**). Once all β-TCP/HA devices had been implanted, muscle tissue pouches with biomaterials were excised using 8 mm biopsy punches (PFM medical, Cologne, Germany). Nine muscle pouches with β-TCP/HA were created, and divided into 3 culturing periods set at 5, 15 and 30 days. Each culturing period

contained 3 tissue pouches. Muscle tissue without β-TCP/HA devices was cultured in parallel to tissue pouches and acted as controls. Medium was changed every 2 days. Fresh muscle tissue was used in the normalization of qRT-PCR.

After the allotted culturing period, specimens with β-TCP/HA devices were harvested and cut in half, with one-half flash frozen in liquid nitrogen for qRT-PCR assays and the other half fixed in 4% paraformaldehyde (Microcos GmbH, Garching, Germany) to be processed for histological and histomorphometric analysis.

3.1.3 Bacterial contamination assay

To determine if tissue cultures systems were contaminated by bacteria and as such have affected histological interpretations, the culture medium was collected after every medium change and randomly tested. Under sterile conditions collected culture medium was plated out on a standard Luria Broth Agar (LA) plates (1g Tryptone, 1.5g Technical agar, 0.5g Yeast extract, 0.5g NaCl (all (Sigma-Aldrich)) in 100ml dH_2O), with a normal LA plate with fresh DMEM-hg (Biochrom GmbH) medium set as control. After 72 hours of incubation at 37 °C with 5% CO_2, plates were assessed for bacterial colony formation by two blinded analysts.

3.1.4 QRT-PCR

QRT-PCR was performed to determine the relative gene expression quantity of tissue growth related genes especially angiogenesis and endothelial tissue formation genes, *VEGF-A* and *COL4A1* and *TGF-β₁* including known osteogenesis signaling and structural markers, specifically *RUNX-2* and *BMP-2*.

Specimen fragments for qRT-PCR were ground to powder in the presence of liquid Nitrogen. Total ribose nucleic acid (RNA) was then isolated using a modified RNA Trizol extraction procedure (Chomczynski & Mackey, 1995). Briefly, 1 ml Trizol (Invitrogen, San Diego, CA, USA) was added to the powderised tissue, where through the addition of chloroform (Sigma-Aldrich) the aqueous RNA containing phase was transferred to Isopropanol (Sigma-Aldrich). RNA was then pelleted out in an overnight centrifugation step at 4 °C, which were then washed with 75% ethanol dried and resuspended in 32 µl RNase free water. The concentration of the RNA was determined using a NanoDrop^{TM}Lite (Thermo Scientific, Waltham, USA) and quality assessed with a Bioanalyzer 2100 (Agilent Technologies, CA, USA). RNA integrity numbers lower than 8 were not accepted. RNA was then reverse transcribed into complementary DNA (cDNA) using the QuantiTect Reverse Transcription cDNA Synthesis Kit (Qiagen, Hilden, Germany).

QRT-PCR was then performed, in duplicate with FastStart Essential DNA Green Master (Roche, Basel, Switzerland) in a final reaction volume of 10 µl, using a LightCycler$^®$ 96 thermocycler (Roche). Each reaction contained 10 ng cDNA; 2x FastStart Essential DNA Green Master and 10 µM of each primer (**Table 1**). Primers were designed using Integrated DNA Technologies PrimerQuest Tool (https://eu.idtdna.com/Primerquest/Home/Index). Use of GeNorm (http://medgen.ugent.be/~jvdesomp/genorm/) established that *ribosomal protein large P0 (RPLP0)*, *succinate dehydrogenase complex subunit A (SDHA), RNA polymerase II subunit E (POLR2E)* and *TATA binding protein (TBP)* were the most appropriate internal reference genes to use in this experiment. All amplified PCR (polymerase chain reactions) products underwent Sanger sequencing (GATC Biotech,

Cologne, Germany) and were then analyzed utilizing nucleotide analysis (https://blast.ncbi.nlm.nih.gov/Blast.cgi?PAGE_TYPE=BlastSearch) to confirm that the correct sequence had been amplified. QRT-PCR thermocycling parameters included a pre-incubation of 3 min at 95°C, followed by a three-step amplification program of 40 cycles consisting of a denaturation, annealing and extension step set at 95°C for 10 s, 60 °C for 15s and 72°C for 30s, respectively. Relative gene expression was normalized against four reference genes. Gene expression from the harvested tissue/device models was normalized to the four reference genes and fresh abdominal skeletal muscle tissue using the Qbase+ software (http://www.biogazelle.com). Gene expression results were represented as mean calibrated normalized relative quantities (CNRQs) ± SEM, which reflect the $\log_{10} 2^{-\Delta\Delta Ct}$.

Table 1. Gene primer sequences for target and reference genes in the pilot study.

Gene	Forward Primer (5´-3´)	Reverse Primer (5´-3´)
VEGF-A	CTACCAGCGCAGCTATTG	GATCCGCATGATCTGCATAG
COL4A1	CTGGGAATCCCGGACTT	GGGATCTCCCTTCATTCCT
TGF-β₁	TTTAGGAAGGACCTGGGTT	ACCCACGTAGTAGACGATG
BMP-2	GGAAGTGGCCCACTTAGA	TCACTAGCAGTGGTCTTACC
RUNX-2	CCCAAGTGGCCACTTAC	CTGAGGCGGTCAGAGA
RPLP0 (reference)	CAACCCAGCTCTGGAGA	CAGCTGGCACCTTATTGG
SDHA (reference)	GCGGTATGACACCAGTTATT	CCTGGCAAGGTAAACCAG
POLR2E (reference)	GACCATCAAGGTGTACTGC	CAGCTCCTGCTGTAGAAAC

| *TBP* | TAACCCAGAAAGTCGAAGAC | CCGTAAGGCATCATTGGA |
| *(reference)* | | |

3.1.5 Quantitative angio-/vasculogenic protein assays

The amount of VEGF-A produced by the two bioreactors and controls were determined using Magnetic Luminex® Assays (R&D systems, Minneapolis, USA). Supernatants of tissue cultures were harvested at 5 days, 15 days and 30 days for either the wrapping model specimens or the pouch model specimens and controls. VEGF-A contents in supernatants were measured according to the manufacturer's instructions. Results were generated using xPONENT® 4.2 for MAGPIX® Software (R&D systems, Minneapolis, USA).

3.1.6 Histological and histo-morphometrical evaluation

Specimens were fixed in 4% paraformaldehyde (Microcos GmbH) for 24h after which they were processed for paraffin wax embedding. Prior to cutting 10μm sections the surface of each paraffin block was decalcified (Bancroft and Gamble, 2008). In order to validate our gene expression patterns with respect to tissue survivability within the two tissue models, histological sections were stained using either the hematoxylin and eosin (HE, Morphisto GmbH, Frankfurt, Germany) staining (Feldman and Wolfe, 2014) or the Movat (Morphisto GmbH) pentachrome staining (Movat, 1955). Stained sections were subsequently analyzed under PreciPoint M8 microscope (PreciPoint, Freising, Germany).

Histomorphometric analysis was performed using Image-Pro Plus v7 (Media Cybernetics, Inc., Rockville, USA). One representative section at the middle of the scaffold from each sample was analysed. Three tissue samples per group were used for histomorphometry. First,

the positively area (PA) within the scaffold and the total area of the scaffold as the region of interest (ROI) were established respectively. Subsequently PA / ROI (%) was calculated and values were demonstrated as a mean percentage of positive area within the scaffold from each group.

3.2 Bone formation by autoinduction *in vitro*

3.2.1 7% HA/CC (coral-derived) devices

Macroporous replicas of coral-derived calcium carbonate exoskeletons of the genus Gonipora were prepared by hydrothermal chemical exchange with phosphate (Ripamonti, 1991; Shors, 1999). Limited conversion to hydroxyapatite resulted in calcium carbonate constructs with 7% hydroxyapatite defined as 7% HA/CC (Biomet, Indiana, USA) (Ripamonti et al., 2010). 7% HA/CC constructs were rods 5 mm in diameter and 3.5 mm in length. The solid components of the HA/CC replica averaged 130 μm in diameter and their interconnections were 220 μm; the average porosity was 600 μm and their interconnections averaged at 260 μm in diameter (Ripamonti, 1991; Shors, 1999).

3.2.2 Muscle pouch organoid culturing model

Four Fischer 344/DuCrl adult male *Rattus norvegicus* (Charles River, Sulzbach, Germany), were utilized in the pilot study, and equally split between the two tissue models. Animals were euthanized with an overdose of isoflurane (Abbot, Chicago, USA). This was done in accordance to the rules and regulations of the Animal Protection Laboratory Animal Regulations (2013), European Directive 2010/63/EU and approved by the Animal ethics research committee (AESC) of the Ludwig Maximillian's University of Munich (LMU), Bavaria, Germany Tierschutzgesetz §1/§4/§17 (https://www.gesetze-im-

internet.de/tierschg/TierSchG.pdf) with respect to animal usage for pure tissue or organ harvest only.

Forty-eight coral-derived 7% HA/CC devices were prepared by placing them in serum-free growth medium as explained in the section of the tissue wrapping model. Rats were then euthanized under sterile conditions, 7% HA/CC devices were immediately implanted in intramuscular pouches created by sharp and blunt dissection (**Figure 4**).
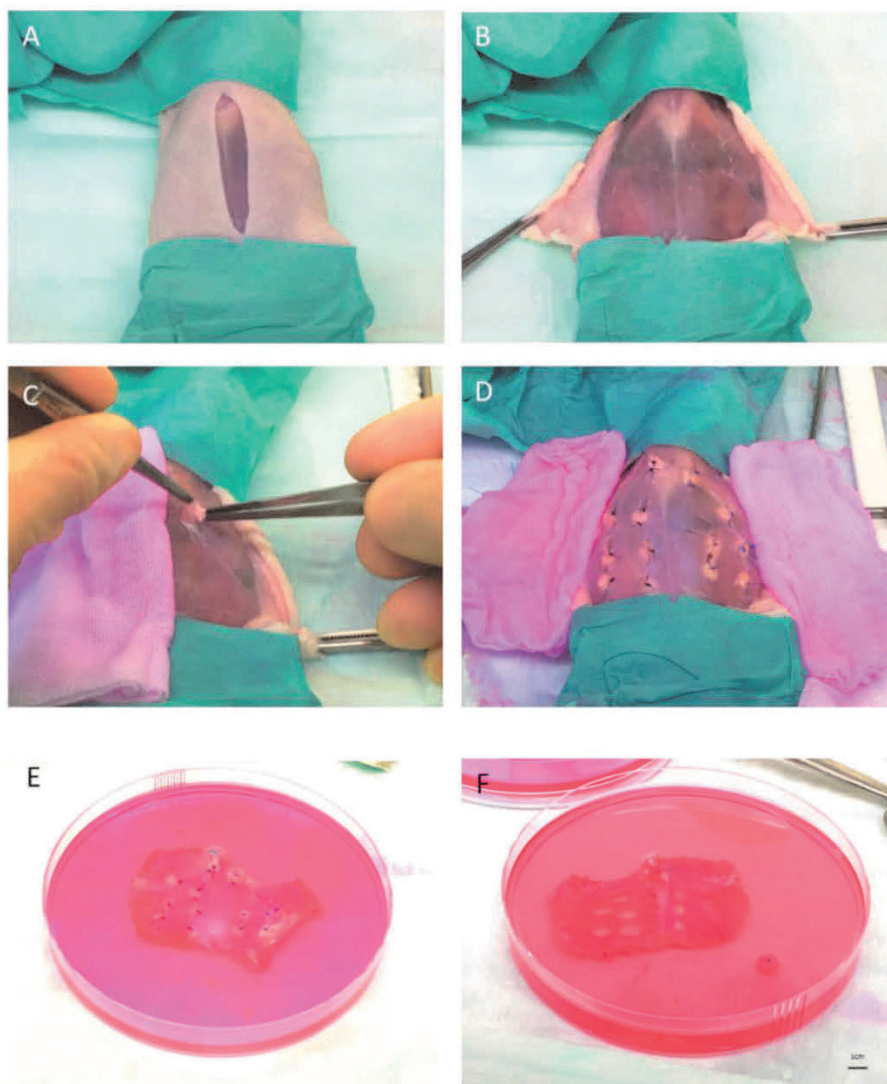
Figure 4. Establishment of *in vitro* 7% HA/CC device -muscle pouch model organoid system.

Once all 7% HA/CC devices had been implanted, muscle tissue pouches with biomaterials were excised using 8 mm biopsy punches (PFM medical). Forty-eight muscle pouches with 7% HA/CC device were created, with half cultured in serum-free growth medium and half cultured in serum-free osteogenic medium (Lennon et al., 1995; Sottile et al., 2003; Heng et al., 2004; Kishimoto et al., 2013; Langenbach and Handschel, 2013; Sinha and Vyavahare, 2013) composed of DMEM-hg, 40 IU/ml penicillin, 40 IU/ml streptomycin, 100 nM dexamethasone (Sigma-Aldrich, St. Louis, MI, USA), 10mM β-glycerophosphate (Sigma-Aldrich), and 50 µM L-ascorbic acid (Sigma-Aldrich), and subsequently divided into 4 culturing periods set at 5, 15, 30 and 60 days. Each treatment group (in either normal growth or osteogenic medium) per culturing period contained 6 tissue pouches. Muscle tissue without 7% HA/CC devices was cultured in parallel to tissue pouches and acted as controls. Medium was changed every 2 days. Fresh muscle tissue was used in the normalization of qRT-PCR.

After the allotted culturing period, specimens with 7% HA/CC device devices were harvested and cut in half, with one-half flash frozen in liquid nitrogen for qRT-PCR assays and the other half fixed in 4% paraformaldehyde (Microcos GmbH, Garching, Germany) to be processed for histological and histomorphometric analysis.

3.2.3 Bacterial contamination assay

To determine if tissue cultures systems were contaminated by bacteria and as such have affected histological interpretations, the culture medium was collected after every medium change and randomly tested. Under sterile conditions collected culture medium was plated out on a standard Luria Broth Agar (LA) plates, with a normal LA plate with fresh DMEM-

hg (Biochrom GmbH) medium set as control. After 72 hours of incubation at 37 °C with 5% CO_2, plates were assessed for bacterial colony formation by two blinded analysts.

3.2.4 QRT-PCR

QRT-PCR was performed to determine the relative gene expression quantity of tissue growth related genes, including *VEGF-A*, *COL4A1, TGF-β1, TGF-β2,* and *TGF-β3,* as well as known chondro-/osteogenesis signaling and structural markers, specifically *RUNX-2, BMP-2, BMP-4, BMP-6, BMP-7, osteocalcin (OCN), alkaline phosphatase (ALP), COL1A1, SOX-9, aggrecan (ACAN), COL2A1, and COL10A1.*

Specimen fragments for qRT-PCR were ground to powder in the presence of liquid Nitrogen. Total RNA was then isolated using a modified RNA Trizol extraction procedure (Chomczynski & Mackey, 1995). Briefly, 1 ml Trizol (Invitrogen, San Diego, CA, USA) was added to the powdered tissue, where through the addition of chloroform (Sigma-Aldrich) the aqueous RNA containing phase was transferred to Isopropanol (Sigma-Aldrich). RNA was then pelleted out in an overnight centrifugation step at 4 °C, which were then washed with 75% ethanol dried and resuspended in 32 µl RNase free water. The concentration of the RNA was determined using a NanoDrop^{TM} Lite (Thermo Scientific, Waltham, USA) and quality assessed with a Bioanalyzer 2100 (Agilent Technologies, CA, USA). RNA integrity numbers lower than 8 were not accepted. RNA was then reverse transcribed into cDNA using the QuantiTect Reverse Transcription cDNA Synthesis Kit (Qiagen).

QRT-PCR was then performed, in duplicate with FastStart Essential DNA Green Master (Roche) in a final reaction volume of 10 µl, using a LightCycler® 96 thermocycler (Roche).

Table 2. Gene primer sequences for target and reference genes in the main study.

Gene	Forward Primer (5´-3´)	Reverse Primer (5´-3´)
VEGF-A	CTACCAGCGCAGCTATTG	GATCCGCATGATCTGCATAG
COL4A1	CTGGGAATCCCGGACTT	GGGATCTCCCTTCATTCCT
TGF-β₁	TTTAGGAAGGACCTGGGTT	ACCCACGTAGTAGACGATG
TGF-β₂	AAATAAGAGCCAAGAGCTGG	GGACTCCAGTCTGTAGGAG
TGF-β₃	AACCTAAGGGTTACTATGCC	ACCACCATGTTGGACAG
RUNX-2	CCCAAGTGGCCACTTAC	CTGAGGCGGTCAGAGA
BMP-2	GGAAGTGGCCCACTTAGA	TCACTAGCAGTGGTCTTACC
BMP-4	TGAGGTGATCTCCTCTGC	ATGGACTAGTCTGGTGTCC
BMP-6	GGACATGGTCATGAGCTTTG	GTCAGAGTCTCTGTGCTGAT
BMP-7	AGGGCTGGTTGGTATTTG	GAAGAAGGCCACCATGAA
COL1A1	GGTGACAGAGGCATAAAGG	AGACCGTTGAGTCCATCT
ALP	CGACAGCAAGCCCAAG	AGACGCCCATACCATCT
OCN	GCGACTCTGAGTCTGACA	GGCAACACATGCCCTAAA
SOX-9	CCAGAGAACGCACATCAAG	GGTGGTCGGTGTAGTCATA
ACAN	CAAGTGGAGCCGTGTTT	GAGCGAAGGTTCTGGATTT
COL2A1	ATCCAGGGCTCCAATGA	AAGGCGTGAGGTCTTCT
COL10A1	CCAGGTCTCAATGGTCCTA	TGTCCAGGCACTCCTTTA
RPLP0 (reference)	CAACCCAGCTCTGGAGA	CAGCTGGCACCTTATTGG
GAPDH (reference)	CATGGGTGTGAACCATGA	TGTCATGGATGACCTTGG
POLR2E (reference)	GACCATCAAGGTGTACTGC	CAGCTCCTGCTGTAGAAAC
ACTB (reference)	AGCTATGAGCTGCCTGA	GGCAGTAATCTCCTTCTGC
TBP (reference)	TAACCCAGAAAGTCGAAGAC	CCGTAAGGCATCATTGGA
RPL13A (reference)	TTTCTCCGAAAGCGGATG	AGGGATCCCATCCAACA

Each reaction contained 10 ng cDNA; 2x FastStart Essential DNA Green Master and 10 µM

of each primer (**Table 2**).

Primers were designed using Integrated DNA Technologies PrimerQuest Tool

(https://eu.idtdna.com/Primerquest/Home/Index). Use of geNorm

(http://medgen.ugent.be/~jvdesomp/genorm/) established that *RPLP0*, *GAPDH*, *POLR2E*,

ACTB, TBP, and *RPL13A* were the most appropriate internal reference genes to use in this

experiment. All amplified PCR products underwent Sanger sequencing (GATC Biotech,

Cologne, Germany) and were then analyzed utilizing nucleotide analysis

(https://blast.ncbi.nlm.nih.gov/Blast.cgi?PAGE_TYPE=BlastSearch) to confirm that the

correct sequence had been amplified. QRT-PCR thermocycling parameters included a pre-

incubation of 3 min at 95°C, followed by a three-step amplification program of 40 cycles

consisting of a denaturation, annealing and extension step set at 95°C for 10 s, 60 °C for 15s

and 72°C for 30s, respectively. Relative gene expression was normalized against six

reference genes. Gene expression from the harvested tissue/device models was normalized

to the six reference genes and fresh abdominal skeletal muscle tissue using the Qbase+

software (http://www.biogazelle.com). Gene expression results were represented as mean

calibrated normalized relative quantities (CNRQs) ± standard error (SEM), which reflect the

$\log_{10} 2^{-\Delta\Delta Ct}$.

3.2.5 Histological and histomorphometrical evaluation

Specimens were fixed in 4% paraformaldehyde (Microcos GmbH) for 24h after which they

were processed for paraffin wax embedding. Prior to cutting 2µm sections the surface of

each paraffin block was decalcified (Bancroft and Gamble, 2008). In order to validate our

gene expression patterns with respect to tissue survivability within the two tissue models, histological sections were stained using either the HE (Morphisto GmbH, Frankfurt, Germany) staining (Feldman and Wolfe, 2014) or the Movat (Morphisto GmbH) pentachrome staining (Movat, 1955). Stained sections were subsequently analyzed under PreciPoint M8 microscope (PreciPoint, Freising, Germany).

Histomorphometric analysis was performed using Image-Pro Plus v7 (Media Cybernetics, Inc., Rockville, USA). One representative section at the middle of the scaffold from each sample was analyzed. Three tissue samples per group were used for histomorphometry. First, the PA within the scaffold and the total area of the scaffold as the region of interest (ROI) were established respectively. Subsequently PA / ROI (%) was calculated and values were demonstrated as a mean percentage of positive area within the scaffold from each group.

3.2.6 Immunohistochemical and immune-histomorphometric assays

For angio-/vasculogenesis and chondro-/osteogenesis evaluation, 2 μm-thick paraffin wax sections were incubated with primary antibody to detect the presence of VEGF-A, COL4A1, ACAN, COL1A1 and OCN. The primary antibody of VEGF-A, COL4A1, ACAN, COL1A1 and OCN (Biorbyt) was diluted by antibody diluent (ZYTOMED SYSTEMS GmbH, Berlin, Germany) at the concentration of 1:200, 1:100, 1:150, 1:200, and 1:100, respectively, determined by serial dilution pre-test with established specimens set as positive control. The Vina Green TM Chromogen Kit (Biocare Medical) was prepared freshly for each protein assay as chromogen to show the antigen-antibody interactions. The sections of the specimens were then analyzed with a PreciPoint M8 microscope with images captured using the Viewpoint software. Green staining of the areas indicated positive protein production.

Accordingly, the absorbance value of the incident light in the blank area of specimens is calibrated. The integrated optical density (IOD) was then measured and the mean optical density (MOD) of ROI was calculated using the following formula: MOD = IOD/ ROI, which represents the corresponding value of the relative strength of antigenicity in the slice.

3.3 Statistical analysis

Data were analyzed using GraphPad Prism v8.0.1 (GraphPad Software, San Diego, USA). The results were represented as mean ± SEM. Measurements were performed in either immune-histomorphometric analysis (n=3) and qRT-PCR (n=6). The Holm-Sidak method was used to detect statistical differences with $\alpha = 0.05$. Statistical significance was indicated by ns for no significance, * for $p<0.05$, ** for $p<0.01$ and *** for $p<0.001$.

CHAPTER 4

RESULTS

4.1 Tissue pouch model supported superior tissue survival than tissue wrapping model

   in vitro

Many investigators have designed 3D osteogenic bioreactors utilizing different sources of

cells and types of scaffolds (Kim and Ma, 2012; Bhumiratana et al., 2016; Tsimbouri et al.,

2017). However, the osteogenic transformation of fibrous tissue *in vitro* is conceived

impossible owing to the lack of a blood supply (Trueta, 1963). This study attempted for the

first time to establish a tissue-scaffold complex *in vitro* that would support tissue

survivability *ex vivo* and cast light on inducing *de novo* bone formation over a long culturing

period, which attempts to replicate the normal *in vivo* experimental environmental conditions

of most known extra-skeletal bone inductive models (Urist and Strates, 1971; Sampath and

Reddi, 1981; Ripamonti, 1991; Klar et al., 2013).

The abdominal skeletal muscle tissue of adult male Fischer 344/DuCrl rats was utilized,

where macro-/microporous β-TCP/HA were either wrapped in the tissue harvested or where

β-TCP/HA devices were first implanted in non-harvested muscle pouch within heterotopic

sites, the standard experimental form to test new bone induction *in vivo*, and then excised

before being cultured *in vitro* (**Figure 3**). In order to test the survivability of these two

models, we pushed the culturing time up to 30 days, where no evidence, to our knowledge,

has yet reported on culturing muscle tissue *ex vivo* for more than 30 days. In the tissue

wrapping model, no gene expression data could be generated for the 30-day *in vitro* β-

TCP/HA wrapped in skeletal muscle tissue from rats (**Figure 5 J, Figure 6 C**), as the tissue

became necrotic, gradually losing the original tissue structure with denuclearization,

preventing successful extraction of messenger ribose nucleic acid (mRNA) to be available

for qRT-PCR analysis (**Figure 5 A-C, Figure 8 A-D**). On the other hand, β-TCP/HA devices

pouched in the skeletal muscle survived the 30-day *in vitro* culturing process (**Figure 5 D-F, J, Figure 8 E-H**), with no bacterial contamination in the culturing system (**Figure 7**). Furthermore, histomorphometric analysis showed a consistent tissue survival around the scaffold in the pouch model up to 30 days, with ongoing tissue necrosis in the wrapping model over time. Statistical difference between these two models was observed at day 30 (P < 0.05) (**Figure 5 G**).
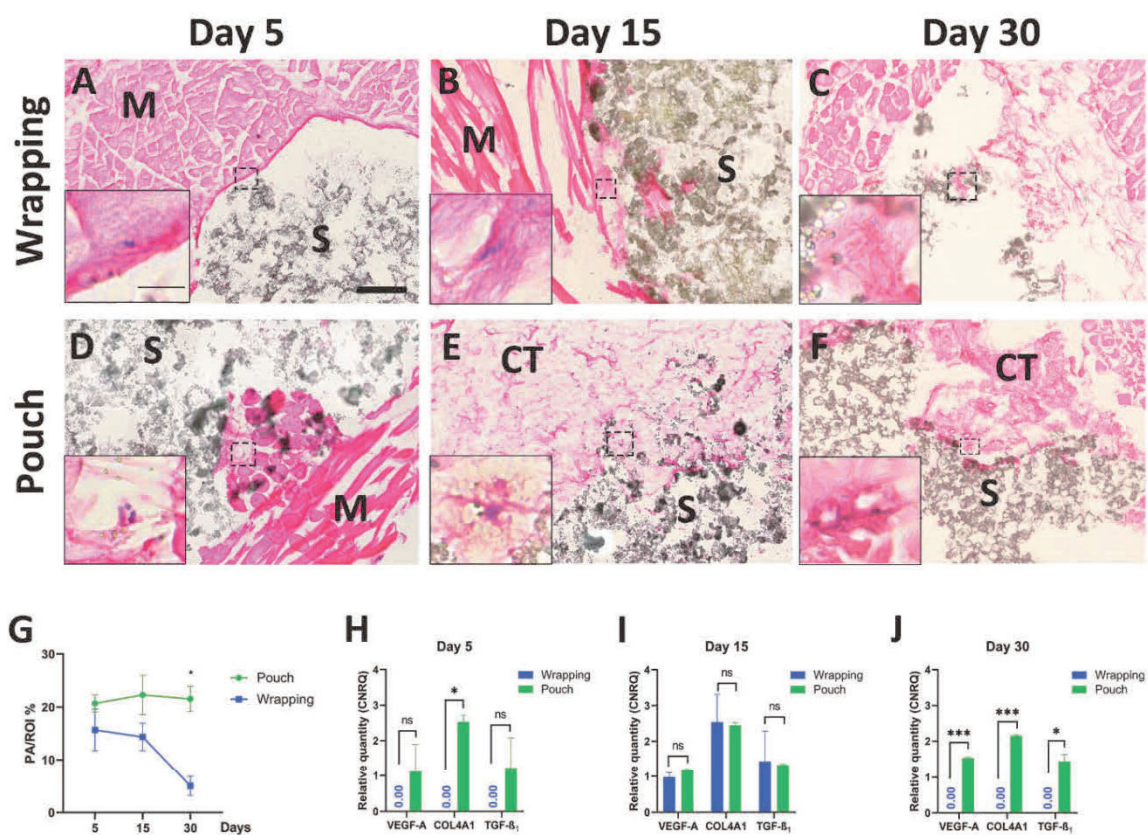
Figure 5. Comparison of tissue survivability between the two in vitro models in growth medium at day 5, 15 and 30 (**A-J**). Cells are confined at the interface between muscle and scaffold at day 5 in the wrapping model (**A**), with a shock silence of tissue-survival related genes (**H**). Muscle tissue undergoes necrosis over time (**B**) with dying of cells (**C, I** and **J**). In the pouch models, initial cell releasing occurs at day 5 (**D**), leading to successive cell migration and connective tissue formation (**E**). Viable vessels (F, higher power view) are still present by day 30 in vitro culturing with consistent tissue survival and growth gene expression pattern. Histological analysis (**G**) shows superior tissue survival around/within the scaffold (P < 0.05) by day 30. Error bars are Mean ± SEM. Ns, non-statistically significant; *, P < 0.05; ***, P < 0.001. HE staining. M = Skeletal muscle, S = scaffold, CT = connective tissue. Bar: Lower power, 200 µm; higher power, 20 µm.

With the goal of defining the difference of gene expression pattern between these two models and evaluate which method provides better tissue growth and survival with possible osteogenic tendencies we then compared the qRT-PCR data between them. The tissue wrapping model, only at day 15 *in vitro* showed an up-regulation of tissue survival and angiogenesis markers including *VEGF-A* and *COL4A1* and *TGF-β₁* (**Figure 5 H-J**), whereas β-TCP/HA bioceramics pouched in abdominal skeletal muscle tissue of rats showed a considerable increase in angiogenesis and endothelial tissue formation genes expression at all timepoints (P < 0.05). For osteogenic differentiation markers, only *BMP-2* up-regulation was noticed at day 5 in the wrapping model (**Figure 6 A**), while both *RUNX-2* and *BMP-2* were steadily up-regulated over time in the pouch model and was superior than the wrapping model at day 30 (P < 0.01) (**Figure 6 A-C**). These results suggest better tissue growth and survivability *in vitro* in a tissue pouch model.
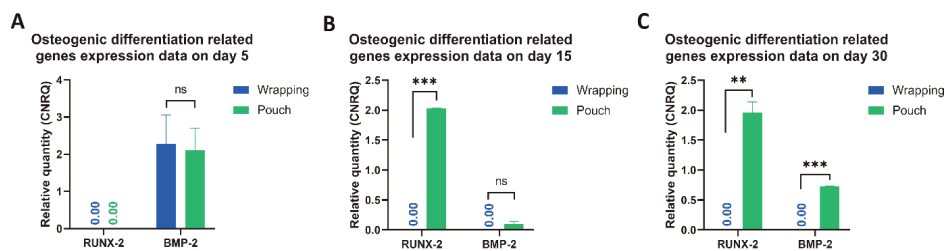
Figure 6. Chronological osteogenic-related gene expression pattern in both wrapping and pouch model (**A - C**). Pouch models showed superior osteogenic differentiation capacity at day 15 (**B**) and 30 (**C**) comparing wrapping models. Error bars are Mean ± SEM. Ns, non-statistically significant; **, P < 0.01; ***, P < 0.001.
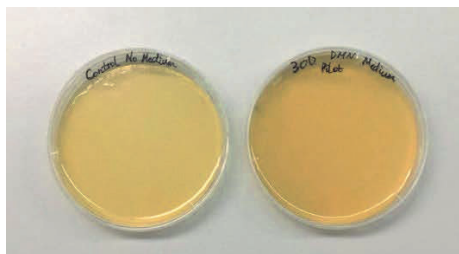
Figure 7. Microbiological culture results of the 30-day culturing medium with a pouch model. No microbial contamination is detected in the 30-day culturing medium with a pouch model (right plate).
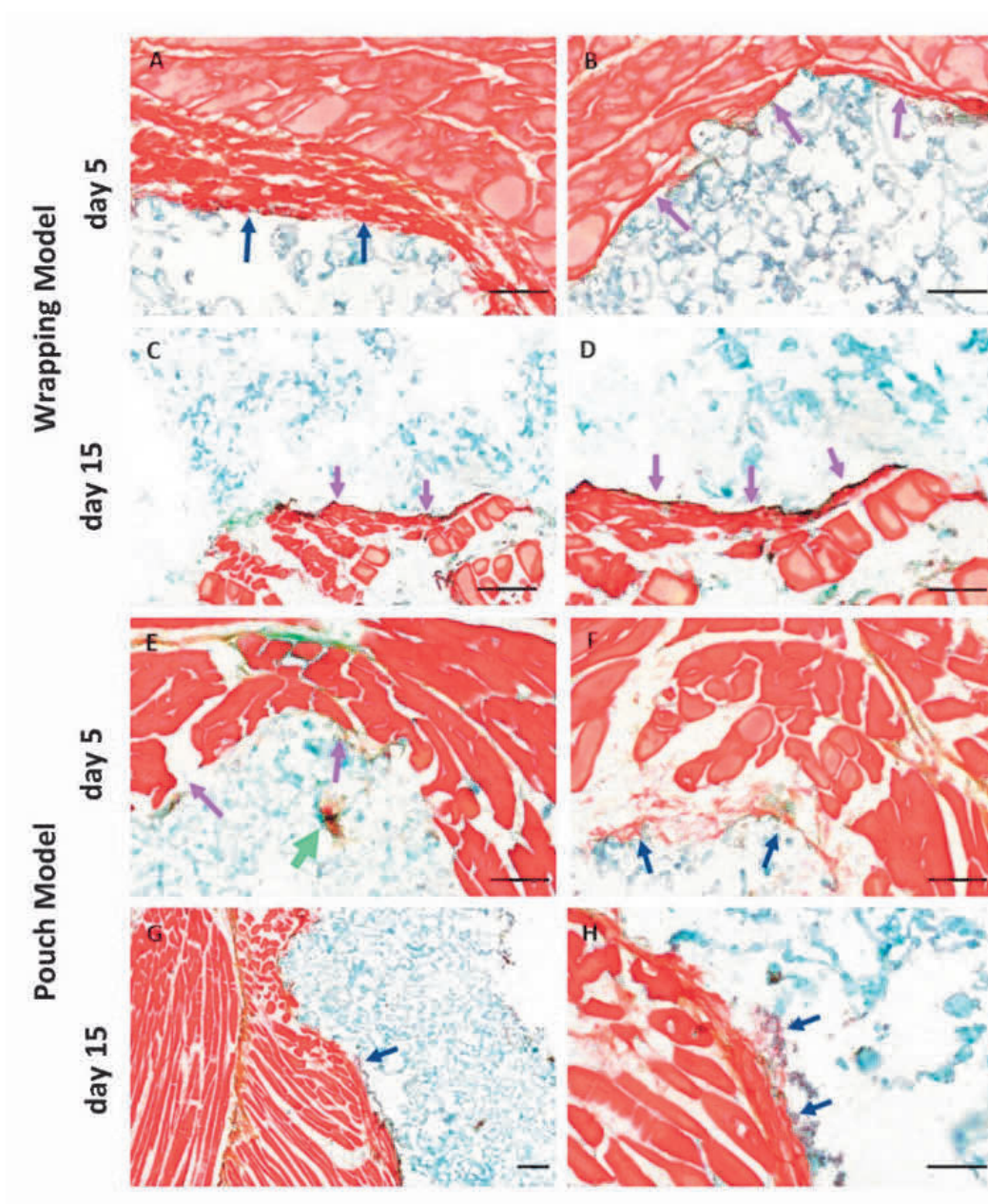
Figure 8. Morphology and tissue response to devices in wrapping models and pouch models at day 5 and day 15 (**A - H**). A considerable amount of fibrils were seen forming into the device (**A, F**; blue arrows) with some collagen-osteoid formation (green arrow) noticeable at days 5, while the self-adaptation of tissue at the periphery of device was observed in both models (B, E; pink arrows). In contrast, to tissue implanted heterotopically (**G, H**; blue arrows) the survivability of tissue was compromised in the tissue bag model at days 15, where the muscle tissue on the periphery of the bioceramic device was observed to undergo a type of fragmentation, discontinuing fibrous tissue formation at the interface of the muscle and device (**C, D**; pink arrows). Movat pentachrome staining was utilized to assess for collagen associated with chondrogenesis and osteogenesis, elastic fibers, muscle and connective tissue. Bars: A, B, D, E, F and H = 100μm; C and G = 200 μm.

4.2 Maintenance of vascular structure in tissue pouch models

Upon demonstrating better tissue survivability and growth in the tissue pouch model through histology/histomorphometry and gene expression patterns representative of cell proliferation and differentiation supporting new tissue formation, the chronological change of *VEGF-A* gene expression, protein production pattern up to 30 days of the culturing process and histological results at day 30 was assessed in the heterotopic pouch model (**Figure 9**). This aimed to determine if a regulatory gene pattern could be identified and prove that this model indeed supports vascular structure maintaining and potential angiogenesis.
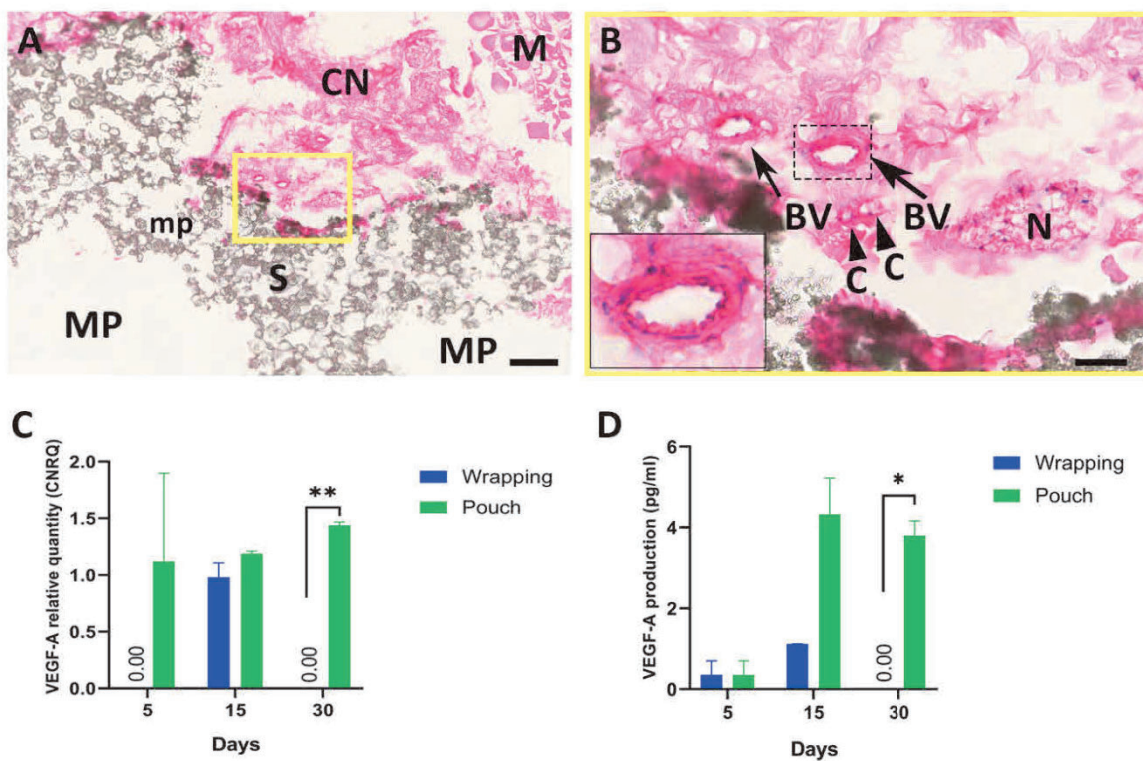
Figure 9. Maintenance of vascular structure and potential of angiogenesis in tissue pouch models up to 30 days (**A-D**). Connective tissue grows into the macropore of the scaffold at the periphery (**A**, dotted lines show the contour of the macropores), with neurovascular bundle still surviving by 30 days (**B**). Both transcriptional (**C**) and translational (**D**) results suggest the maintenance of angiogenesis capacity with a pouch model by 30 days, whereas the capacity loses with a wrapping model (P < 0.01 and 0.05, respectively). Error bars are Mean ± SEM. *, P < 0.05; **, P < 0.01. HE staining. M = Skeletal muscle, S = scaffold, CT = connective tissue, MP = macropores, mp = micropores, BV = blood vessel, N = nerve, C = capillary. Bar: **A**, 200 μm; **B**, 50 μm.

In β-TCP/HA bioceramic devices muscle pouch model, the best up-regulated genes were *COL4A1*, *VEGF-A* and *TGF-β₁* at day 15 and day 30, whilst at day 5 it was *COL4A1*, *BMP-2* and *VEGF-A* (**Figure 5, Figure 6**). In short, *COL4A1* and *VEGF-A* were highly up-regulated at all time-points, whilst a marked high expression of *BMP-2* at day 30 occurred compared with muscle tissue alone ($P < 0.05$) (**Figure 10 I**). Our findings, in the gene expression aspect, suggest that the bioceramic devices muscle pouch support vessel survival and potential angiogenesis when cultured under normal *in vitro* growth conditions with limited osteogenic tendencies present, especially 30 days after treatment.

4.3 Tissue pouch models initiate osteogenic differentiation *ex vivo*

Histological sections of β-TCP/HA bioceramic devices wrapped in rat abdominal skeletal muscle tissue clearly showed a thin layer of fibrous-like tissue lining the interface between muscle tissue and scaffold at day 5 (**Figure 5A**). In contrast, fibrils and cells were released from the injured muscle fibers and attached to the interface of the scaffold (**Figure 5 D**). Successively, a noticeable increase of the volume of necrotic muscle fibers was observed at day 15 in the bioceramic muscle tissue wrapped model (**Figure 5 B**), with limited numbers of condensed nuclei containing fibers sparsely distributed within ECM at the periphery of the devices. In contrast, muscle tissue of the bioceramic devices in the heterotopic pouch model, at day 15, appeared to actively "invade" and undergo a transformation, into connective tissue (**Figure 5 E**) that was clearly visible at the tissue to scaffold microporous interface and could partially be observed lining the macroporous hole-like structures of the scaffold (**Figure 5 E** higher magnification view). By day 30, in contrast to tissue pouched bioceramic devices, as represented in **Figure 5 F**, the survival of tissue was compromised in the wrapping model, where the muscle tissue on the periphery of the bioceramic device was

observed to undergo a type of fragmentation, discontinuing fibrous tissue growth at the muscle to device interface (**Figure 5 C**), without any presence of living cells within the scaffold (**Figure 5 C** higher magnification view). Contrarily, for the 30 days heterotopic pouch model group, the muscle tissue was seen breaking down (**Figure 10 C** and **G**),
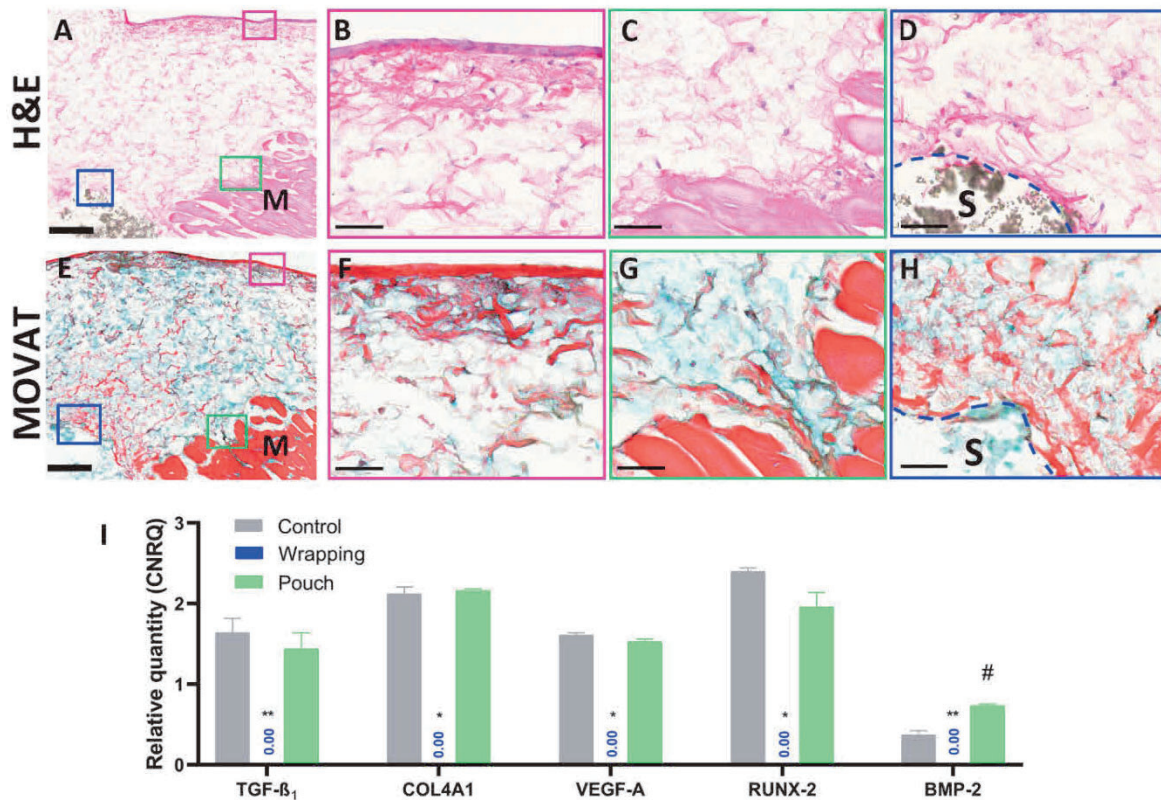
Figure 10. Representative morphology and tissue response to devices in pouch models at day 30 (**A-I**). Extensive connective tissue forms (**A and B**) around the scaffold, with comprehensive mucin deposition (**E** in blue) and fibrils (**E** in red) evenly distributed in between, consistent with the gene expression pattern showing proliferation and angiogenesis (**I**). A fibrous tissue layer forms at the interface contacting medium (**B and F**), where fibrous-like cells line at the surface of tissue (**B**), producing condensed fibers (**F** in red) underneath. Cells releasing from muscle fiber (**C**) migrate within the mucin-fibril rich extracellular matrix (**G**) towards either outer layer or scaffold (**D and H**). The osteoid (**H**, area in scarlet) mesh at the interface (dashed lines) between tissue and scaffold indicates the osteogenic transformation of the connective tissue, which is supported by BMP-2 gene expression results ($P < 0.05$). Error bars are Mean ± SEM. *,#, $P < 0.05$; **, $P < 0.01$. HE staining (**A-D**); Movat pentachrome staining (E-H). M = Skeletal muscle, S = scaffold. Bar: **A** and **E**, 200 µm; **B-D**, **F-H** 50 µm.

yet obviously supporting connective tissue that was observed invading, although mainly at the periphery, into the macroporous superstructure of the β-TCP/HA devices (**Figure 10 D** and **H**), with fibrils also appearing to interact with the particles of the porotic bioceramic scaffold. No cells or tissues pertaining to bone formation could be visualized.

Subsequently, during muscle tissue degeneration, cells within and between the muscle tissue fibers were released and appeared to be migrating into the scaffold together with the extra-cellular matrix (**Figure 10 A, C** and **D**). Certain transitional zone showed some signs of a collagen-osteoid-like matrix forming near the connective tissue to porous superstructure interphase of the device (**Figure 10 E** and **H**). These results indicated that cell migration could be initiated as early as day 5, being supported up to 30 days by connective tissue in the tissue pouch model, with limited formation of collagen-osteoid-like matrices at the peripheries of the porous device.

4.4 Coral devices facilitate cell proliferation and tissue ingrowth

In order to improve the biological response of skeletal muscle tissue to the biomaterial in the pouch model established in our previous proof of concept study, 7% HA/CC device as a proven efficient biomaterial that can spontaneously induce extra-skeletal bone formation in vivo was utilized to replace the β-TCP/HA device. As shown in **Figure 11**, the 7% HA/CC device was surrounded by a layer of approximately 1 mm thick abdominal skeletal muscle (**E**), while a thinner muscle thickness of around 200 μm was made in the β-TCP/HA group (**A**). An early-phase ECM formation was partially present from the periphery to the center of the 7% HA/CC device lining the contour of the macropores and seemingly attempting to fill the pores.
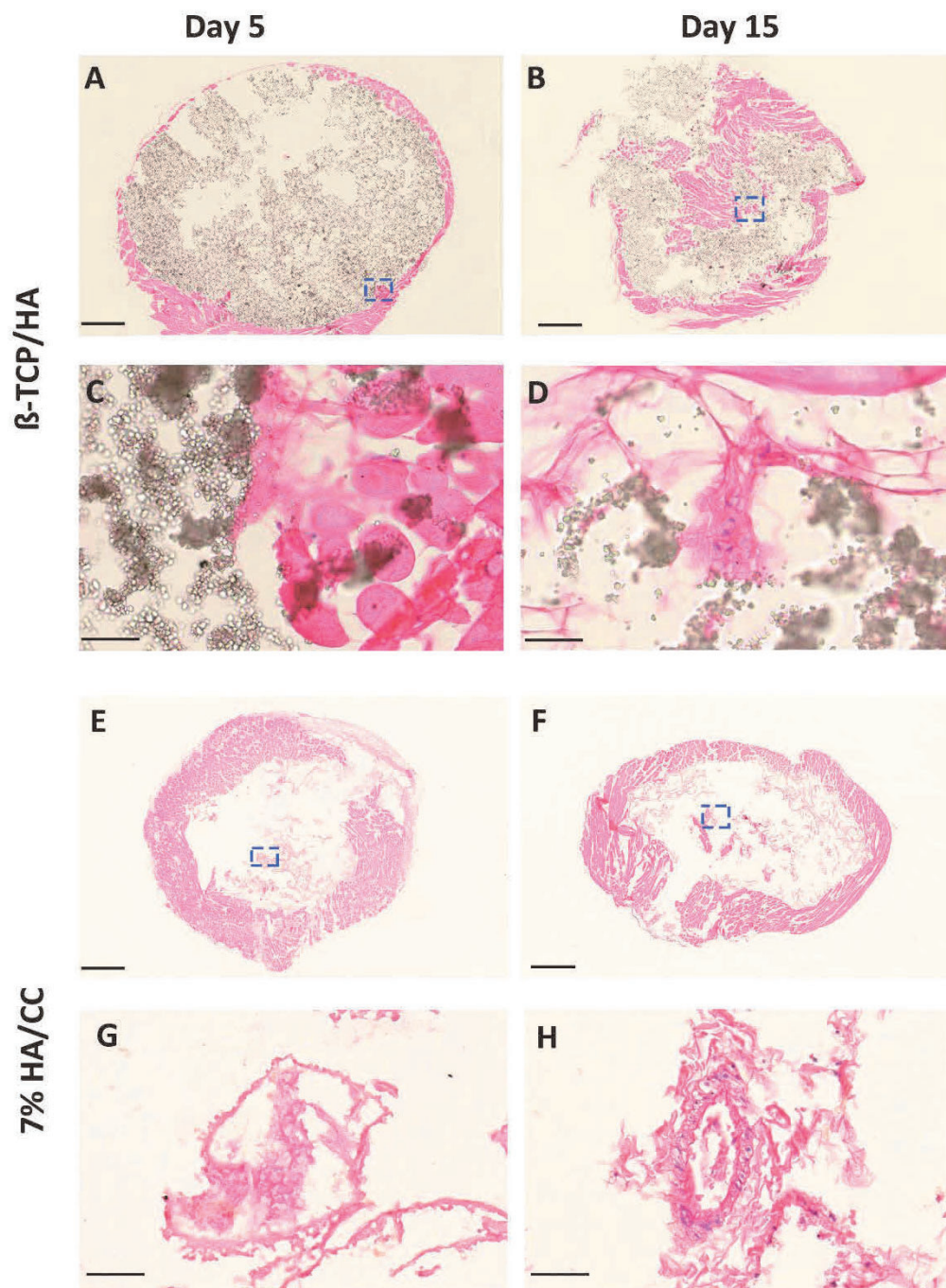
Figure 11. Biological responses to the β-TCP/HA and 7% HA/CC device with a muscle-pouch model by day 15. ECM with the presence of cells are confined at the periphery of the β-TCP/HA device by day 15 (**A - D**), whilst 7% HA/CC device initiates efficient tissue ingrowth into the macropores at day 5 and supports a more comprehensive cell migration by day 15, showing specific structures at the concavities within the device. HE staining (**E – F**). Bar: **A, B, E, F** = 1mm, **C, D, G, H** =50 µm.

In contrary, no tissue could be seen within the β-TCP/HA device at day 15 while fibrous tissue with limited cells were constrained at the periphery of the device (**B** and **D**). In brief, a more efficient ingrowth of connective tissue was induced into the 7% HA/CC device from the very early phase of *in vitro* culturing at day 5 (**E** and **G**), whereas only limited ECM was noticed attached to the interface of peripheral macropores of the β-TCP/HA device without any ECM available within the device (**A** and **C**). By day 15, a more comprehensive tissue ingrowth with clustered cells located in ECM could be noted at the center of the 7% HA/CC device (**F** and **H**).

4.5 7% HA/CC device initiates and mediates angiogenesis and osteogenesis with extended long-term culture

In the 30-day long-term culture, tissue around the device showed active response to the device (**Figure 12 A**), where neurovascular structures (**Figure 12 C**) were still maintained in the 7% HA/CC device -muscle pouch model and mucin and collagen formation was present at the periphery (**Figure 12 E** and **G**). The culture period was further extended up to 60 days and a more comprehensive tissue formation within the macroporous structures was noted in histochemical evaluation (**Figure 12 B**). Still, intact vascular structure was shown in the muscle tissue after the 60-day culturing with the thickening of the mucin formation (**Figure 12 D** and **F**). Furthermore, mucin and fibrous-like tissue combined with erythrocyte was demonstrated lining at the interface of the concavity at the center of the 7% HA/CC device (**Figure 12 H**).
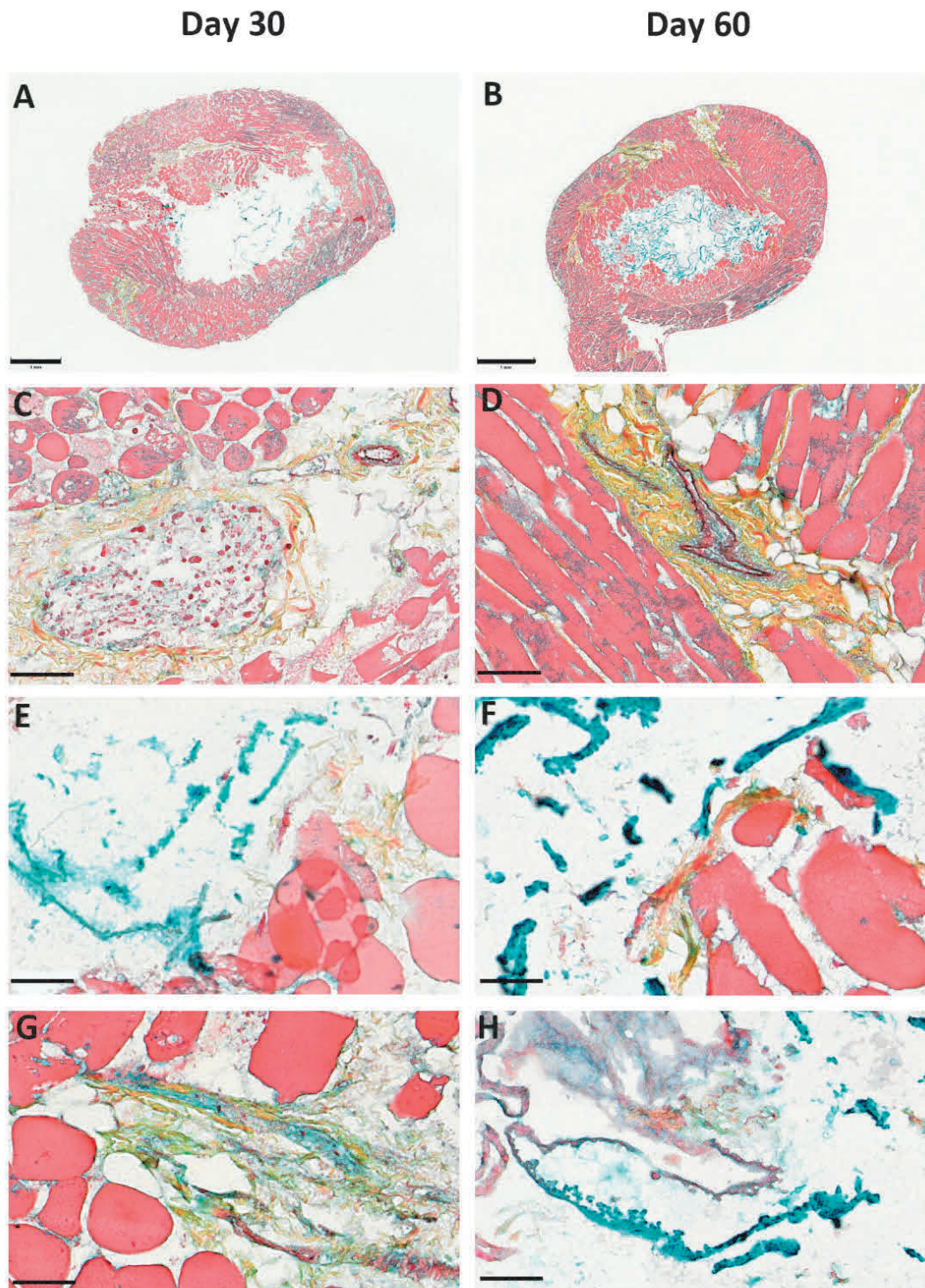
Figure 12. Morphology of tissue around and within 7% HA/CC device at day 30 and 60 (**A - H**). Movat pentachrome staining was utilized to assess for collagen associated with chondrogenesis and osteogenesis, elastic fibers, muscle and mucin.

The angiogenic potential within this system was further investigated using either qRT-PCR or immunohistological assays. *COL4A1* as a known prerequisite marker for angiogenesis, reflecting basal membrane formation was regulated over time, reached the climax at day 15 and then significantly being down-regulated by day 60 (**Figure 13 E**).
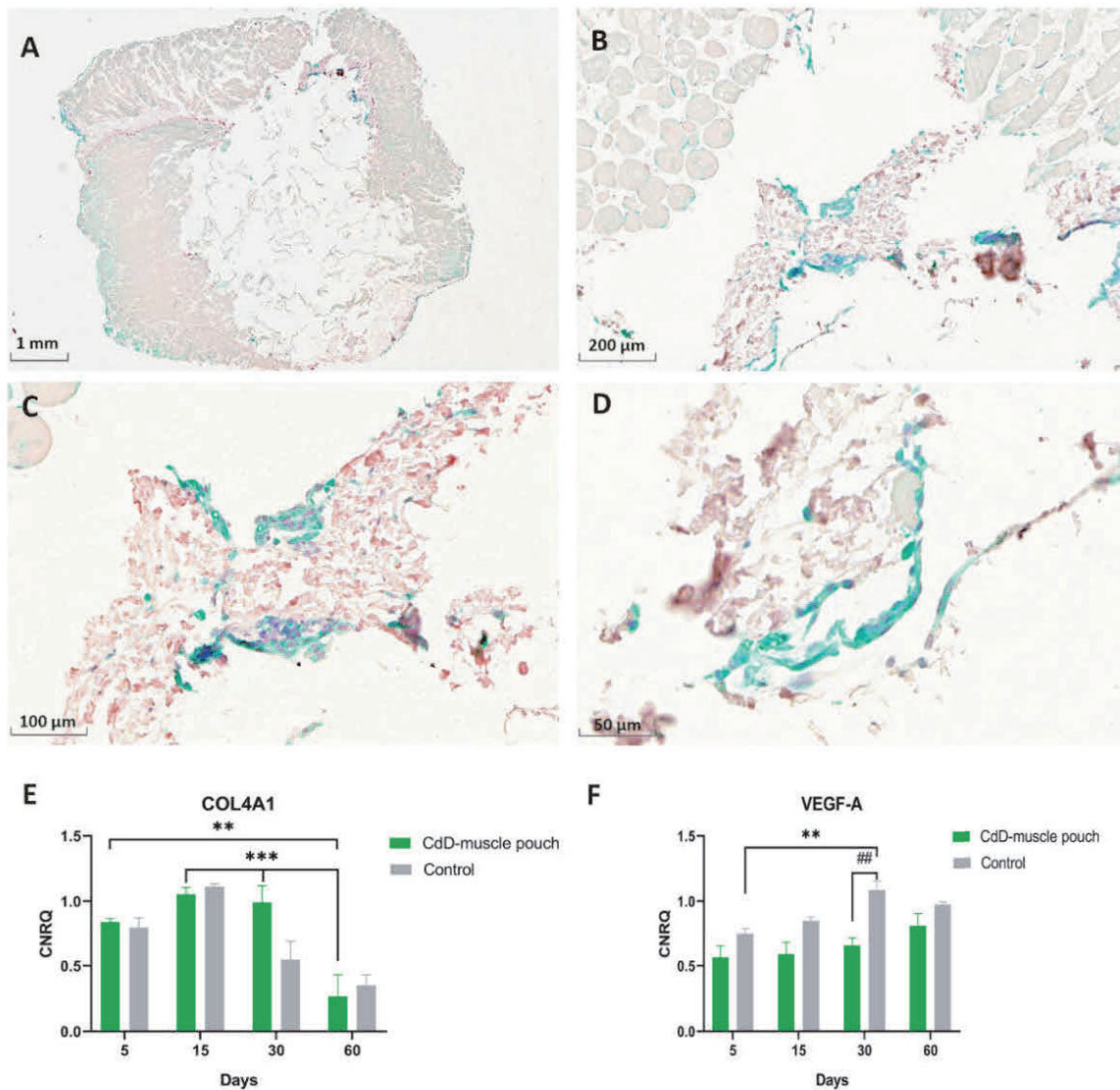
Figure 13. Immunohistological analysis of VEGF-A protein expression within the 7% HA/CC device in the biomaterial-muscle pouch model by day 60 (**A** – **D**) and angiogenic gene markers expression pattern over time (**E** – **F**). Error bars are Mean ± SEM. Two-way ANOVA and Turkey's multiple comparison are used to detect statistical significance (n=6). ** and ##, $P < 0.01$; ***, $P < 0.001$.

Besides, compared with muscle tissue alone, its potential for angiogenesis was maintained with no statistically significant difference. In terms of VEGF-A, a down-stream angiogenic marker that has been most commonly used for evaluating angiogenesis, demonstrated a steadily increasing up-regulation in the 7% HA/CC device -muscle system, whilst the peak up-regulation was reached at day 30 in muscle alone. Significant difference was only present at day 30 between 7% HA/CC device -muscle system and muscle alone. (**Figure 13 F**) Immunohistological staining of VEGF-A at day 60 (**Figure 13 A - D**) showed that VEGF-A protein production was mainly located at the surface of the macropores within the device, with some vascular-like structure actively expressing VEGF-A. In short, an extended long-term culture facilitated the angiogenesis process with the 7% HA/CC device -muscle pouch organoid system.

For osteogenesis, osteoid tissue formation was seen within the 7% HA/CC device device at day 60, while immunohistological assays of OCN, an important marker for mineralisation, showed a significant increase either histomorphologically or histomorphometricallly (**Figure 14 A** and **B**). The gene expression of OCN also confirmed this pattern but without statistical significance (**Figure 14 C**). A constant up-regulation of *RUNX-2*, *SOX-9*, *BMP-2* and *BMP-6* supported the osteogenic differentiation process taking place within the 7% HA/CC device -muscle pouch system (**Figure 14 D**), in which *RUNX-2* and *SOX-9* were markers for the early phase of osteogenic progenitor commitment while *BMP-2* and *BMP-6* were more involved in osteoblast lineage differentiation and mineralisation. Furthermore, the consistent upregulation of *COL1A1* (bone matrix marker) over time accompanied with persistent down-regulation of *COL2A1* (cartilage matrix marker) and *COL10A1* (hypertrophic cartilage marker) suggested an intramembranous ossification process rather

than an endochondral ossification mechanism. (**Figure 15**).
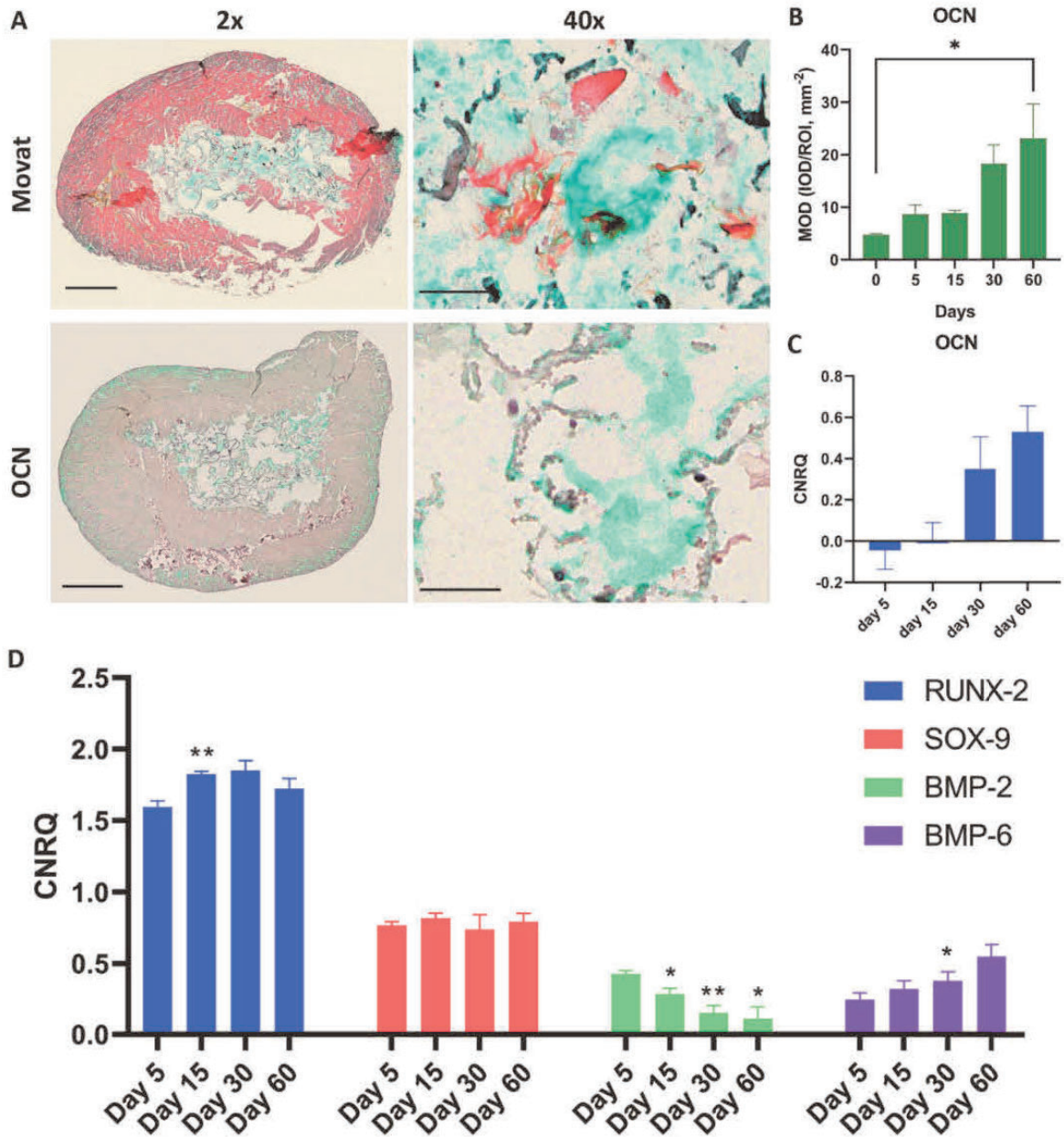
Figure 14. Representative morphology and osteogenic gene markers expression with the 7% HA/CC device -muscle pouch model at day 60 (**A** – **D**).). Error bars are Mean ± SEM. Student t-test is used in histomorphometric analysis of OCN protein production. Two-way ANOVA and Turkey's multiple comparison are used in gene expression data to detect statistical significance at each time point compared with day 5 per gene (n=6). *, $P < 0.05$; **, $P < 0.01$.
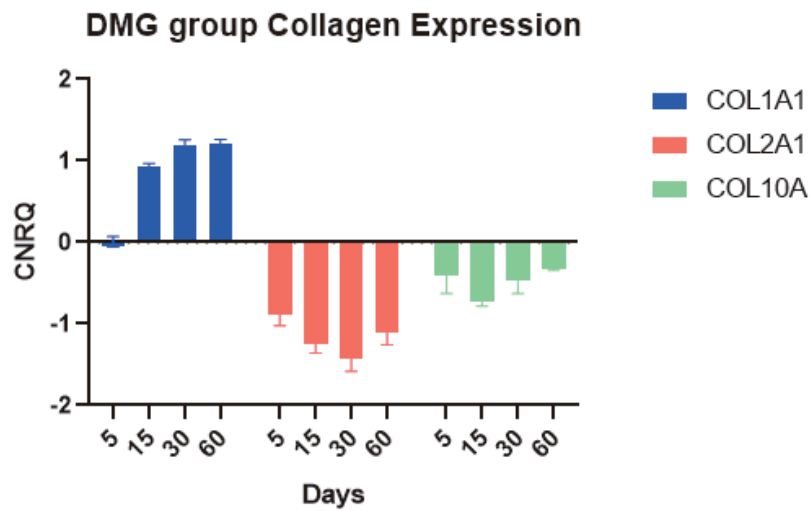
Figure 15. Different collagen types gene expression patterns over time in the muscle-biomaterial organoid pouch model cultured in growth medium. *COL1A1* (blue bars) is consistently and increasingly upregulated, whilst both *COL2A1* and *COL10A1* are constantly down-regulated. Error bars are Mean ± SEM.

4.6 "Osteogenic" medium inhibits angio-/vasculogenesis and accelerates hypertrophic tissue deterioration in extended-period culture.

The effect of previously established osteogenic medium was assessed. Histochemical results showed the collapse of the 7% HA/CC device -muscle system cultured in osteogenic medium with fragmented and disassociated muscle tissue after 60-day culturing (**Figure 16 A**), while the 7% HA/CC device -muscle system maintained intact. A more comprehensive VEGF-A protein expression was shown within the confine of the device by immuno-histological results. Quantitative analysis of both COL4A1 and VEGF-A protein expression, though not statistically significant, exhibited a higher level in the growth medium group comparing the osteogenic medium group. (**Figure 16 B** and **C**)
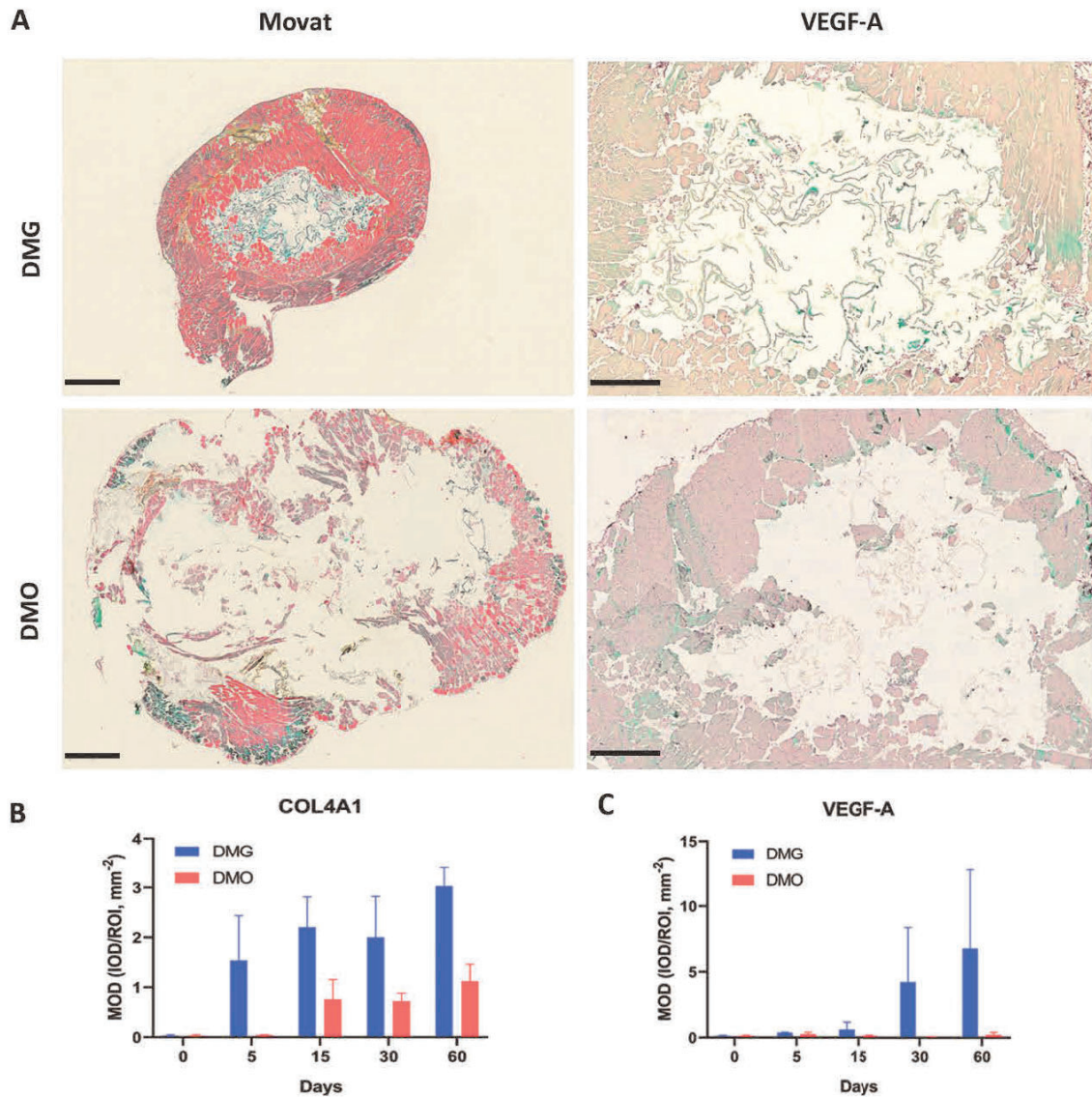
Figure 16. Comparison of histological morphology between 7% HA/CC device-muscle organoid pouch models cultured in growth medium and osteogenic medium by 60 days. Bar: A left panel = 1 mm, right panel = 500 μm. Error bars are Mean ± SEM. DMG, device-muscle cultured in growth medium; DMO, device-muscle cultured in osteogenic medium.

Tissue-survival-related genes including *TGF-β₁*, *VEGF-A* and *COL4A1* was superiorly up-regulated in the growth medium group, indicating a better survival over the 7% HA/CC device -muscle complex cultured in the osteogenic medium. (**Figure 17 A - C**) In contrary, *BMP-2*,

ALP, *OCN,* markers for ossification and mineralization are more up-regulated in the osteogenic

medium group. Concerning the histological morphology of the muscle around and tissue within

the 7% HA/CC device cultured in the osteogenic medium at day 60, the mineralisation related

genes' higher up-regulation indicated a hypertrophic deterioration of tissue when cultured in

the osteogenic medium.
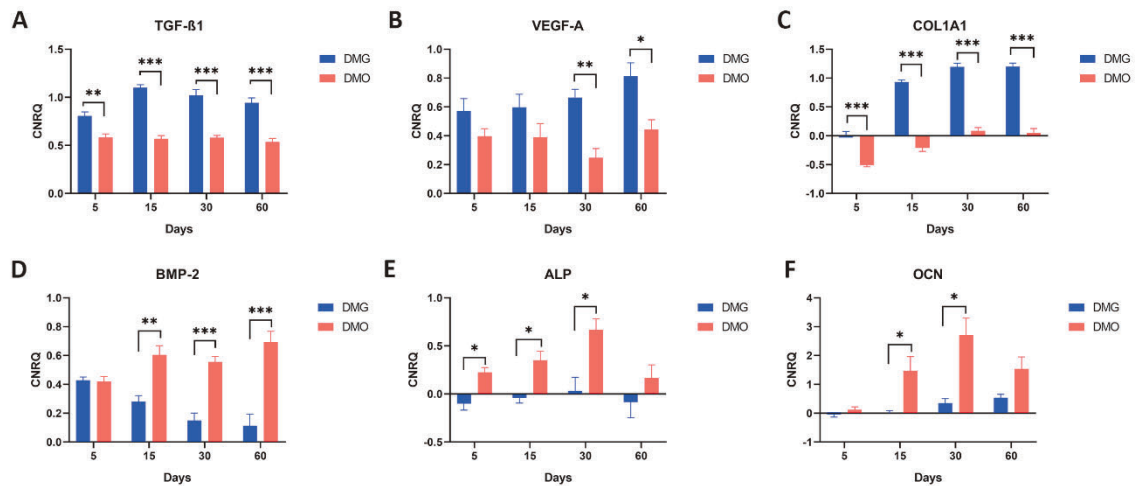
Figure 17. Comparison of genes expression patterns between 7% HA/CC device-muscle organoid pouch models cultured in growth medium and osteogenic medium. Error bars are Mean ± SEM. Two-way ANOVA and Turkey's multiple comparison are used to detect statistical significance (n=6). *, $P < 0.05$; **, $P < 0.01$; ***, $P < 0.001$. DMG, device-muscle cultured in growth medium; DMO, device-muscle cultured in osteogenic medium.

CHAPTER 5

DISCUSSION

5.1 Challenges of translation in tissue engineering and regeneration

Developing a new technology that can fully replicate, synthetically, an *in vivo* environment *in vitro*, however challenging, is attractive as it would allow for more efficient testing on par with the physiological reality of the clinical setting. It is expected that such medically supportive platforms would deliver faster and superior results with reduced costs whilst allowing for more accurate prediction and therapeutic models to be developed for a clinical setting (Freeman et al., 2017). Whilst one solution to this problem has been the emergence of bioreactor platforms (Martin et al., 2004; Plunkett and O'Brien, 2011; Liu et al., 2013; Bouet et al., 2015) that have a limited capacity at replicating some *in vivo* processes, developing a synthetic system that can fully replicate the supra-organ of bone(s), let alone induce bone formation *in vitro*, with its plethora of varying proteins arranged geometrically within the 3D superstructure and assortment of cellular entities (Liu et al., 2013; Klar, 2018) remains perhaps the most challenging prospect for tissue engineering regenerative sciences with only the neurological complexities of the brain surpassing this endeavor.

5.2 Bone tissue engineering and regeneration

The bone tissue engineering paradigm dictates that bone tissue induction and morphogenesis rely on the principles that soluble molecular signal(s) combined with an insoluble substratum are critical for the initiation and formation of *de novo* bone tissue *in vivo* (Urist et al., 1967; Sampath and Reddi, 1981). A further prerequisite, in order to facilitate proper bone formation to occur, is that of an adequate vascular supply, formed either by vasculogenesis and/or angiogenesis, with vessel structures invading the macro- and microporous superstructure of a device and bringing vital stem cells, nutrients, amino acids, protein signals and other resources. This would culminate in new endothelial tissue invasion into the

confines of the substratum, supplying nutrients necessary for subsequent new bone tissue formation (Trueta, 1963; Polykandriotis et al., 2007; Beier et al., 2010). However, it was never shown what happens when there is no vascular supply or angiogenesis to bring new material for biological constructive process, such as was the case in the present pilot study *in vitro*.

Vasculogenesis is classically defined as the differentiation of precursor cells, angioblasts, into endothelial cells and the new formation of a primitive vascular network, whereas angiogenesis is the formation of new capillaries from an existing arterial or venous blood vessel (Vailhé et al., 2001). Various 2D and 3D *in vitro* models have been previously developed to replicate vasculo-/angiogenesis *in vitro* and investigate key characteristics that would help in understanding and directing these processes better as *in vivo* (Arthur et al., 1998; Wartenberg et al., 1998; Goumans et al., 1999; Zhu et al., 2000). The pioneering assays often utilizing embryonically derived stem cells, endothelial cells and/or cancer cells in conjunction with some fibrin, collagen type I and other matrices (Auler et al., 2017) remain instrumental applications that provided insights into the formation of vascular and angiogenic structures at an *in vitro* level. However, to date actual tissue vasculogenesis or even angiogenesis from harvested tissue for use within *in vitro* based tissue regenerative procedures, especially to help establish a bone formation bioreactor system as was tested within the present study, remains a pioneering novelty.

5.3 A biomaterial-muscle pouch model organoid system

In the present study, *COL4A1* was originally chosen as it is a well-known biomarker for angiogenesis, where it is critical in the basement membrane formation of new capillaries and

partially also in endothelial tissue development (Reddi, 2000; Ripamonti, 2006; Klar et al., 2014). *VEGF-A* was included after interest was aroused at whether angiogenesis would also be developed, as it is known to support the endothelial tissue formation and act as a paracrine signaling molecule on the development and proliferation of endothelial cells, especially during new osteogenesis (Mayer et al., 2005). Interestingly, qRT-PCR analysis and histological observations in our proof-of-concept study revealed that *COL4A1* and *VEGF-A* are only briefly up-regulated within the wrapping model at day 15, after which the tissue died off in tissue culture. On the other hand, the β-TCP/HA device pouched in abdominal skeletal muscle sites, harvested and then cultured *in vitro,* showed a consistent and almost regulatory pattern of endothelium proliferation and/or angiogenesis up to 30 days at either transcriptional or translational level. This could also, at least for connective and endothelial-like tissue formation and invasion into the β-TCP/HA printed bioceramics, be validated histologically. Here new tissue formation was histologically apparent by day 30, invading the macroporous superstructure of the devices, near the peripheries only. Moreover, whilst true osteogenesis eluded our investigations, as this was not a central aim as yet at this point, the gene expression level of *RUNX-2* increased considerably at both day 15 and 30 in the pouch groups with also positive up-regulation of *BMP-2 and TGF-β₁*. This suggests that the presently utilized pouch model has the potential to form new bone at an *in vitro* cell culturing level, as it was demonstrated to do *in vivo* in various animal models (Urist, 1965). However, possibly because of the reduced stem cell availability, the resident differentiated osteoblastic cells present within the pouch model were too low to facilitate proper bone formation in the *in vitro* model. This is perhaps due to lack of an active blood supply that would normally bring in extra stem cells and even monocyte/macrophages critical for osteoclastogenesis (Klar et al., 2013) and which are an essential support for new bone formation. Alternatively,

the bioceramic devices used might not have been of a sufficient quality to fully support the spontaneous induction of new bone formation signals. Multiple studies reported that interconnection pathway has a strong impact on osteogenic outcomes, with incomplete and undersized pore interconnection limiting efficient connective tissue infiltration and blood vessels invasion into the scaffold (Mastrogiacomo et al., 2006). However, in our proof of concept study, the average diameter of the interconnection pathway was ~40 μm, indicating the limited capacity for sound tissue and vascular invasion, subsequently constrained the proper bone formation within the micropores. This could explain why connective tissue formation and vascular survival were only observed in this study at the peripheral macropores with diameter larger than 500 μm. In the 7% HA/CC device study, the ingrowth of tissue into the device was significantly improved with an extended culture time up to 60 days. Furthermore, the angiogenic and osteogenic differentiation potential was noted within this device. The results from our 7% HA/CC device study again support the theory concerning the pores interconnection pathway pattern, because the 7% HA/CC device has wider interconnection pathway allowing cells as well as ECM to migrate and grow into the center of the device. The present results showed promising prospect of this organoid system with 7% HA/CC device, but still, this leaves new strategic avenues open to improve the responsive signals in the system and the formation of *de novo* bone *in vitro*. Follow-up experiments need to be considered to investigate this aspect further, by using established biomimetic devices that are known to be viable at inducing bone formation spontaneously.

Aside from the initial validations of the *in vitro* pouch model as a tissue model to be utilized for further investigations with good survival chances, partial osteogenic support combined with angiogenic responses, our study revealed new connective tissue formation and

endothelial tissue survival at the peripheral region of the heterotopic pouch implanted devices. This indicates that *in vitro* blood vessel had survived the long-term culture period with resident cells producing the necessary signals that are required for tissue survival with the potential to angiogenesis that could support connective tissue ingrowth into the scaffold and the subsequent osteogenic differentiation of MSCs located within the connective tissue. We postulate that the surrounding tissue in heterotopic sites are actively engaged in the formation of specific connective and/or endothelial tissue formation rather than simply providing a signal that facilitates an immunological response or acting as a stem cell reservoir to sustain the metabolic formation of new bone by induction with an insoluble substratum (Urist, 1965; Sampath and Reddi, 1981; Klar et al., 2013; Klar et al., 2014; Ripamonti et al., 2016).

Various researches into *in vitro* metabolic effects of cells removed from their natural environment and cultured with an *ex vivo* system clearly re-iterate that cells lose their homeostatic state where critical essential amino acid building blocks, normally available for protein synthesis, suddenly disappear. This greatly limits efficient protein translation (Nelson and Cox, 2005), including losing critical energy production requirements to fuel necessary anabolic activities to support formation of complex ECM components (Cassim et al., 2017). Catabolic reactions using glucose, adipose tissue or proteins are a necessary requirement for the survival of any cell, let alone a tissue. *In vitro* systems cannot adequately replicate these reactions and might prevent cellular *in vitro* tissue experiments from progressing past the generally accepted 30-day culturing period limit (Griffith et al., 2005; Bonab et al., 2006; McKee and Chaudhry, 2017). After this, because of extensive proliferation of cells or tissues, the catabolic breakdown into basic components and energy

might be insufficient to meet the anabolic synthetic requirements to maintain cells and/or tissues active *in vitro* and might therefore limit their capacity to form larger complex organs. However, considering the histological results of the present study of the skeletal muscle pouched bioceramic device cultured *in vitro* up to 60 days, we propose that the muscle tissue rescues the catabolic and anabolic homeostasis by behaving as a catabolic reservoir that breaks down into base components. It has come into consensus that critical components such as extra glucose and proteins but critically essential amino acid, critical for mammalian protein production (Brand, 1997; Albert, 2005; Nelson and Cox, 2005), are released that assists in establishing a new homeostasis *in vitro.* This allows resident stem cells to undergo differentiation and proliferation into the macroporous spaces of the bioceramic device, depositing new endothelial tissue matrix that could support vascular structures. There the culturing medium might act as a nutrient source to more effectively transport biochemical building blocks and nutrients into the confines of the device.

Providing sufficient survival, the tissue *in vitro* could lead to new bone formation by fine tune of the system. This form of cell differentiation and tissue repurposing or "hypertrophic tissue transformation" needs to be further validated and elucidated if it indeed is some type of tissue "recycling" *modus* or is simply an artefact of deterioration. Future research needs to more critically investigate this aspect. Similarly, the benefit of tissue *in vitro* culturing over standard cell culture systems still need to be assessed; we suspect it is so, as the tissue might more efficiently support critical catabolic and anabolic mechanisms as well as more complex cytological reactions, leading to the new *in vitro* formation of complex super organoid bone. In the hereby presented study, the first nascent steps towards developing such a bone inductive/formative environmental reality *in vitro* have been attempted. Systematic

studies can be further developed and improved to ultimately produce *in vitro* bone formation of any skeletal bone in view of clinical applications.

5.4 Outlook for bone formation by autoinduction *in vitro*

There are several aspects that should be further addressed in the future studies. First, osteoclast, with its integral role in bone tissue formation, could be introduced into this system to offer the essential and proper transcriptional and/or translational regulation of the bone formation by introduction *in vitro*. Second, the *in vitro* culturing environment should be further optimized. The first attempt of preparing the culture medium offering a proper milieu for osteoinduction and osteochondral differentiation was made by (Lennon et al., 1995). In the following two decades more efforts are added in this field, trying to optimize the formula of chemicals and proteins to enhance the effect of osteoinduction *in vitro*. (Sottile et al., 2003; Heng et al., 2004; Griffith et al., 2005; Fiorentini et al., 2011; Kim and Ma, 2012; Kishimoto et al., 2013; Langenbach and Handschel, 2013; Sinha and Vyavahare, 2013; Sorice et al., 2014; Freeman et al., 2017; Katagiri et al., 2017; McKee and Chaudhry, 2017; Vrselja et al., 2019) Multiple osteogenic inducers have been investigated where glucocorticoid dexamethasone (anti-inflammation factor), ascorbic acid (ECM promoter) and β-glycerophosphate (mineralization promoter) are considered among the most critical components for the induction of osteogenesis mainly based on *in vitro* stem cells related evidence. (Sottile et al., 2003; Fiorentini et al., 2011; Kishimoto et al., 2013; Langenbach and Handschel, 2013; Sorice et al., 2014) However, debates consist concerning the validity and safety of this formula, owing to its inhibitory effect on angiogenesis and the potential risk of oncogenicity. (McCluskey and Gutteridge, 1982; Yuen et al., 2008; Fan et al., 2014; Bian et al., 2015; Luedi et al., 2018). Particularly, dexamethasone should be taken carefully

as an osteogenic inducer in the *in vitro* culturing. Besides, other inducers like physiologic mediators, including IGF-1, VEGF-A and TGF-β_1 have recently been investigated. (Katagiri et al., 2017) In addition to chemical factors, the mechanical extracellular environment, perfusion microenvironment and diffusion limit are drawing cumulative attention for a more natural and efficient osteogenic *in vitro* culturing environment. (Griffith et al., 2005; Kim and Ma, 2012; Freeman et al., 2017)

Although it has a potential benefit at the very early stage of culturing to facilitate the cell commitment into the osteoblast lineage, its negative effect on tissue survival and angiogenesis dominates in the long-term culture. Third, other types of connective tissue such as periosteum and muscle fascia, thanks to their intrinsic properties of osteogenic metamorphosis potential, could also be investigated as alternatives for a better biological response to bioceramic devices within the tissue-biomaterial organoid system. Last but not least, *in vivo* experiment is a must in the future to 1) validate the spontaneous bone induction effect of the coral-derived macroporous biomaterial in rat; 2) elucidate the conundrum of heterotopic bone induction and formation by biomaterial *in vivo* and subsequently define the direction how to finely tune this *in vitro* tissue-biomaterial complex system for the real bone formation *ex vivo*.

CHAPTER 6

CONCLUSIONS

In conclusion, the proof-of-concept study clearly showed that a pouch model exhibited superior tissue survivability with the maintenance of neurovascular structure *in vitro* compared with the wrapping model, thereby being suitable for follow-up bone inductive endeavors provided the correct material and/or signals are present to facilitate this reaction. The introduction of 7% HA/CC device into the organoid pouch model system facilitated the cell migration and connective tissue penetration into the macropores of the device, subsequently enhancing either the angiogenic or the osteogenic cell differentiation and tissue morphogenesis. Furthermore, extended long-term *in vitro* culture enabled comprehensive ECM network to form within the biomaterial-muscle system, where multiple cell types (MSCs/MPCs, pre-osteoblast, endothelium cells, etc.) essential for initiating real bone formation distributed properly, functioning as a hopeful platform for bone diseases related pharmaceutical investigation. Moreover, as a promising bone graft substitute, this organoid system maintains the long-term survivability of neurovascular structure for a superior capability to connect the neural and vascular network *in situ* of the host compared with to date cell-biomaterial based graft. Additionally, the previously described "osteogenic" medium acted as more of a role accelerating the hypertrophic deterioration of tissue rather than a real enhancement of the bone induction process. In brief, whilst the *in vitro* tissue inductive model can support the development in part of an angiogenic response, the culturing system needs to be further supplemented and enhanced with either the relevant stem cells including monocytes/macrophages lineage uniting a synthetic perfusion system that would enable future *in vitro* models to function as an *in vivo* system would. Subsequently, differences in molecular signals between *in vitro* and *in vivo* pouch models, including macro and micro signals involved in new autogenous bone formation, still need to be determined that would enable such future models to fully replicate the *in vivo* environment ex vivo.

Reference

Albert, R. (2005). Scale-free networks in cell biology. *J Cell Sci* 118(Pt 21), 4947-4957. doi: 10.1242/jcs.02714.

Alexander, P.G., Gottardi, R., Lin, H., Lozito, T.P., and Tuan, R.S. (2014). Three-dimensional osteogenic and chondrogenic systems to model osteochondral physiology and degenerative joint diseases. *Exp Biol Med (Maywood)* 239(9), 1080-1095. doi: 10.1177/1535370214539232.

Amini, A.R., Laurencin, C.T., and Nukavarapu, S.P. (2012). Differential analysis of peripheral blood- and bone marrow-derived endothelial progenitor cells for enhanced vascularization in bone tissue engineering. *J Orthop Res* 30(9), 1507-1515. doi: 10.1002/jor.22097.

Anderer, U., and Libera, J. (2002). In vitro engineering of human autogenous cartilage. *J Bone Miner Res* 17(8), 1420-1429. doi: 10.1359/jbmr.2002.17.8.1420.

Arthur, W.T., Vernon, R.B., Sage, E.H., and Reed, M.J. (1998). Growth factors reverse the impaired sprouting of microvessels from aged mice. *Microvasc Res* 55(3), 260-270. doi: 10.1006/mvre.1998.2078.

Atef, M., Osman, A.H., and Hakam, M. (2019). Autogenous interpositional block graft vs onlay graft for horizontal ridge augmentation in the mandible. *Clin Implant Dent Relat Res*. doi: 10.1111/cid.12809.

Auler, M., Pitzler, L., Pöschl, E., Zhou, Z., and Brachvogel, B. (2017). *Mimicking Angiogenesis in vitro: Three-dimensional Co-culture of Vascular Endothelial Cells and Perivascular Cells in Collagen Type I Gels.*

Bancroft, J.D., and Gamble, M. (2008). *Theory and Practice of Histological Techniques.* Churchill Livingstone.

Beier, J.P., Horch, R.E., Hess, A., Arkudas, A., Heinrich, J., Loew, J., et al. (2010). Axial vascularization of a large volume calcium phosphate ceramic bone substitute in the sheep AV loop model. *J Tissue Eng Regen Med* 4(3), 216-223. doi: 10.1002/term.229.

Betz, R.R. (2002). Limitations of autograft and allograft: new synthetic solutions. *Orthopedics* 25(5 Suppl), s561-570.

Bhatt, R.S., and Atkins, M.B. (2014). Molecular pathways: can activin-like kinase pathway inhibition enhance the limited efficacy of VEGF inhibitors? *Clin Cancer Res* 20(11), 2838-2845. doi: 10.1158/1078-0432.CCR-13-2788.

Bhumiratana, S., Bernhard, J.C., Alfi, D.M., Yeager, K., Eton, R.E., Bova, J., et al. (2016). Tissue-engineered autologous grafts for facial bone reconstruction. *Sci Transl Med* 8(343), 343ra383. doi: 10.1126/scitranslmed.aad5904.

Bian, Y., Qian, W., Li, H., Zhao, R.C., Shan, W.X., and Weng, X. (2015). Pathogenesis of glucocorticoid-induced avascular necrosis: A microarray analysis of gene expression in vitro. *Int J Mol Med* 36(3), 678-684. doi: 10.3892/ijmm.2015.2273.

Blair, H.C., Larrouture, Q.C., Li, Y., Lin, H., Beer-Stoltz, D., Liu, L., et al. (2017). Osteoblast Differentiation and Bone Matrix Formation In Vivo and In Vitro. *Tissue Eng Part B Rev* 23(3), 268-280. doi: 10.1089/ten.TEB.2016.0454.

Bonab, M.M., Alimoghaddam, K., Talebian, F., Ghaffari, S.H., Ghavamzadeh, A., and Nikbin, B. (2006). Aging of mesenchymal stem cell in vitro. *BMC Cell Biol* 7, 14. doi: 10.1186/1471-2121-7-14.

Boos, A.M., Loew, J.S., Deschler, G., Arkudas, A., Bleiziffer, O., Gulle, H., et al. (2011). Directly auto-transplanted mesenchymal stem cells induce bone formation in a ceramic bone substitute in an ectopic sheep model. *J Cell Mol Med* 15(6), 1364-1378. doi: 10.1111/j.1582-4934.2010.01131.x.

Bouet, G., Cruel, M., Laurent, C., Vico, L., Malaval, L., and Marchat, D. (2015). Validation of an in vitro 3D bone culture model with perfused and mechanically stressed ceramic scaffold. *Eur Cell Mater* 29, 250-266; discussion 266-257.

Reference

Boyde, A., Corsi, A., Quarto, R., Cancedda, R., and Bianco, P. (1999). Osteoconduction in large macroporous hydroxyapatite ceramic implants: evidence for a complementary integration and disintegration mechanism. *Bone* 24(6)**,** 579-589.

Brand, M.D. (1997). Regulation analysis of energy metabolism. *J Exp Biol* 200(Pt 2)**,** 193-202.

Cassim, S., Raymond, V.A., Lapierre, P., and Bilodeau, M. (2017). From in vivo to in vitro: Major metabolic alterations take place in hepatocytes during and following isolation. *PLoS One* 12(12)**,** e0190366. doi: 10.1371/journal.pone.0190366.

Chang, B.S., Lee, C.K., Hong, K.S., Youn, H.J., Ryu, H.S., Chung, S.S., et al. (2000). Osteoconduction at porous hydroxyapatite with various pore configurations. *Biomaterials* 21(12)**,** 1291-1298.

Collier, R. (2009). "Rapidly rising clinical trial costs worry researchers". Can Med Assoc).

Cosar, M., Ozer, A.F., Iplikcioglu, A.C., Oktenoglu, T., Kosdere, S., Sasani, M., et al. (2008). The results of beta-tricalcium phosphate coated hydroxyapatite (beta-TCP/HA) grafts for interbody fusion after anterior cervical discectomy. *J Spinal Disord Tech* 21(6)**,** 436-441. doi: 10.1097/BSD.0b013e318157d365.

Costa, J.B., Pereira, H., Espregueira-Mendes, J., Khang, G., Oliveira, J.M., and Reis, R.L. (2017). Tissue engineering in orthopaedic sports medicine: current concepts. *Journal of ISAKOS: Joint Disorders &amp; Orthopaedic Sports Medicine* 2(2)**,** 60. doi: 10.1136/jisakos-2016-000080.

Cox, K., Holtrop, M., D'Alessandro, J., Wang, E., Wozney, J., and Rosen, V. (1991). Histological and ultrastructural comparison of the in vivo activities of rhBMP-2 and rhBMP-5. *J Bone Miner Res* 6(Suppl 1)**,** 155.

D'alessandro, J. (1991). Purification, characterization, and activities of recombinant bone morphogenetic protein 5. *J Bone Miner Res* 6**,** S153.

Daculsi, G., LeGeros, R.Z., Nery, E., Lynch, K., and Kerebel, B. (1989). Transformation of biphasic calcium phosphate ceramics in vivo: ultrastructural and physicochemical characterization. *J Biomed Mater Res* 23(8)**,** 883-894. doi: 10.1002/jbm.820230806.

De La Vega, R.E., De Padilla, C.L., Trujillo, M., Quirk, N., Porter, R.M., Evans, C.H., et al. (2018). Contribution of Implanted, Genetically Modified Muscle Progenitor Cells Expressing BMP-2 to New Bone Formation in a Rat Osseous Defect. *Mol Ther* 26(1)**,** 208-218. doi: 10.1016/j.ymthe.2017.10.001.

De Oliveira, J.F., De Aguiar, P.F., Rossi, A.M., and Soares, G.A. (2003). Effect of process parameters on the characteristics of porous calcium phosphate ceramics for bone tissue scaffolds. *Artif Organs* 27(5)**,** 406-411.

Denayer, T., Stöhr, T., and Van Roy, M. (2014). Animal models in translational medicine: Validation and prediction. *New Horizons in Translational Medicine* 2(1)**,** 5-11. doi: https://doi.org/10.1016/j.nhtm.2014.08.001.

Dey, B.K., Pfeifer, K., and Dutta, A. (2014). The H19 long noncoding RNA gives rise to microRNAs miR-675-3p and miR-675-5p to promote skeletal muscle differentiation and regeneration. *Genes Dev* 28(5)**,** 491-501. doi: 10.1101/gad.234419.113.

Dong, J., Kojima, H., Uemura, T., Kikuchi, M., Tateishi, T., and Tanaka, J. (2001). In vivo evaluation of a novel porous hydroxyapatite to sustain osteogenesis of transplanted bone marrow-derived osteoblastic cells. *J Biomed Mater Res* 57(2)**,** 208-216.

Dong, J., Uemura, T., Shirasaki, Y., and Tateishi, T. (2002). Promotion of bone formation using highly pure porous beta-TCP combined with bone marrow-derived osteoprogenitor cells. *Biomaterials* 23(23)**,** 4493-4502.

Dudek, K.A., Lafont, J.E., Martinez-Sanchez, A., and Murphy, C.L. (2010). Type II collagen expression is regulated by tissue-specific miR-675 in human articular chondrocytes. *J Biol Chem* 285(32)**,** 24381-24387. doi: 10.1074/jbc.M110.111328.

Evans, C.H., and Stoddart, M.J. (2016). Why does bone have TERM limits? *Injury* 47(6)**,** 1159-1161. doi: 10.1016/j.injury.2016.05.004.

Fan, Z., Sehm, T., Rauh, M., Buchfelder, M., Eyupoglu, I.Y., and Savaskan, N.E. (2014). Dexamethasone alleviates tumor-associated brain damage and angiogenesis. *PLoS One* 9(4)**,** e93264. doi: 10.1371/journal.pone.0093264.

Feder, J., Marasa, J.C., and Olander, J.V. (1983). The formation of capillary-like tubes by calf aortic endothelial cells grown in vitro. *J Cell Physiol* 116(1)**,** 1-6. doi: 10.1002/jcp.1041160102.

Feldman, A.T., and Wolfe, D. (2014). Tissue processing and hematoxylin and eosin staining. *Methods Mol Biol* 1180**,** 31-43. doi: 10.1007/978-1-4939-1050-2_3.

Filipowska, J., Tomaszewski, K.A., Niedzwiedzki, L., Walocha, J.A., and Niedzwiedzki, T. (2017). The role of vasculature in bone development, regeneration and proper systemic functioning. *Angiogenesis* 20(3)**,** 291-302. doi: 10.1007/s10456-017-9541-1.

Fiorentini, E., Granchi, D., Leonardi, E., Baldini, N., and Ciapetti, G. (2011). Effects of osteogenic differentiation inducers on in vitro expanded adult mesenchymal stromal cells. *Int J Artif Organs* 34(10)**,** 998-1011. doi: 10.5301/ijao.5000001.

Flamme, I., Baranowski, A., and Risau, W. (1993). A new model of vasculogenesis and angiogenesis in vitro as compared with vascular growth in the avian area vasculosa. *Anat Rec* 237(1)**,** 49-57. doi: 10.1002/ar.1092370106.

Flamme, I., and Risau, W. (1992). Induction of vasculogenesis and hematopoiesis in vitro. *Development* 116(2)**,** 435-439.

Flautre, B., Anselme, K., Delecourt, C., Lu, J., Hardouin, P., and Descamps, M. (1999). Histological aspects in bone regeneration of an association with porous hydroxyapatite and bone marrow cells. *J Mater Sci Mater Med* 10(12)**,** 811-814.

Freeman, F.E., Schiavi, J., Brennan, M.A., Owens, P., Layrolle, P., and McNamara, L.M. (2017). (*) Mimicking the Biochemical and Mechanical Extracellular Environment of the Endochondral Ossification Process to Enhance the In Vitro Mineralization Potential of Human Mesenchymal Stem Cells. *Tissue Eng Part A* 23(23-24)**,** 1466-1478. doi: 10.1089/ten.TEA.2017.0052.

Friedenstein, A. (1968). Induction of bone tissue by transitional epithelium. *Clinical Orthopaedics and Related Research (1976-2007)* 59**,** 21-38.

Friedlaender, G.E., Perry, C.R., Cole, J.D., Cook, S.D., Cierny, G., Muschler, G.F., et al. (2001). Osteogenic protein-1 (bone morphogenetic protein-7) in the treatment of tibial nonunions. *J Bone Joint Surg Am* 83-A Suppl 1(Pt 2)**,** S151-158.

Fujimura, K., Bessho, K., Okubo, Y., Segami, N., and Iizuka, T. (2003). A bioactive bone cement containing Bis-GMA resin and A-W glass-ceramic as an augmentation graft material on mandibular bone. *Clin Oral Implants Res* 14(5)**,** 659-667.

Galindo-Moreno, P., Avila, G., Fernandez-Barbero, J.E., Mesa, F., O'Valle-Ravassa, F., and Wang, H.L. (2008). Clinical and histologic comparison of two different composite grafts for sinus augmentation: a pilot clinical trial. *Clin Oral Implants Res* 19(8)**,** 755-759. doi: 10.1111/j.1600-0501.2008.01536.x.

Garrison, K.R., Donell, S., Ryder, J., Shemilt, I., Mugford, M., Harvey, I., et al. (2007). Clinical effectiveness and cost-effectiveness of bone morphogenetic proteins in the non-healing of fractures and spinal fusion: a systematic review. *Health Technol Assess* 11(30)**,** 1-150, iii-iv.

Gauthier, O., Bouler, J.M., Aguado, E., Pilet, P., and Daculsi, G. (1998). Macroporous biphasic calcium phosphate ceramics: influence of macropore diameter and macroporosity percentage on bone ingrowth. *Biomaterials* 19(1-3)**,** 133-139.

Gauthier, O., Muller, R., von Stechow, D., Lamy, B., Weiss, P., Bouler, J.M., et al. (2005). In vivo bone regeneration with injectable calcium phosphate biomaterial: a three-dimensional micro-computed tomographic, biomechanical and SEM study. *Biomaterials* 26(27)**,** 5444-5453. doi: 10.1016/j.biomaterials.2005.01.072.

Gilbert, S.F. (2000). *Developmental Biology - Osteogenesis: The Development of Bones 6th edition.* Sunderland, MA: Sinauer Associates.

Gonda, K., Nakaoka, T., Yoshimura, K., Otawara-Hamamoto, Y., and Harrii, K. (2000). Heterotopic ossification of degenerating rat skeletal muscle induced by adenovirus-mediated transfer of

bone morphogenetic protein-2 gene. *J Bone Miner Res* 15(6)**,** 1056-1065. doi: 10.1359/jbmr.2000.15.6.1056.

Goumans, M.J., Zwijsen, A., van Rooijen, M.A., Huylebroeck, D., Roelen, B.A., and Mummery, C.L. (1999). Transforming growth factor-beta signalling in extraembryonic mesoderm is required for yolk sac vasculogenesis in mice. *Development* 126(16)**,** 3473-3483.

Govender, S., Csimma, C., Genant, H.K., Valentin-Opran, A., Amit, Y., Arbel, R., et al. (2002). Recombinant human bone morphogenetic protein-2 for treatment of open tibial fractures: a prospective, controlled, randomized study of four hundred and fifty patients. *J Bone Joint Surg Am* 84(12)**,** 2123-2134. doi: 10.2106/00004623-200212000-00001.

Griffith, C.K., Miller, C., Sainson, R.C., Calvert, J.W., Jeon, N.L., Hughes, C.C., et al. (2005). Diffusion limits of an in vitro thick prevascularized tissue. *Tissue Eng* 11(1-2)**,** 257-266. doi: 10.1089/ten.2005.11.257.

Gu, Z., Xie, H., Li, L., Zhang, X., Liu, F., and Yu, X. (2013). Application of strontium-doped calcium polyphosphate scaffold on angiogenesis for bone tissue engineering. *J Mater Sci Mater Med* 24(5)**,** 1251-1260. doi: 10.1007/s10856-013-4891-8.

Hammonds, R.G., Jr., Schwall, R., Dudley, A., Berkemeier, L., Lai, C., Lee, J., et al. (1991). Bone-inducing activity of mature BMP-2b produced from a hybrid BMP-2a/2b precursor. *Mol Endocrinol* 5(1)**,** 149-155. doi: 10.1210/mend-5-1-149.

Havers, C., and Geuder, M.F. (1692). *Osteologia nova: sive, Novae quaedam observationes de ossibus, et partibus ad illa pertinentibus.* Apud Georgium Wilhelmum Kühnium.

He, T., Cao, C., Xu, Z., Li, G., Cao, H., Liu, X., et al. (2017). A comparison of micro-CT and histomorphometry for evaluation of osseointegration of PEO-coated titanium implants in a rat model. *Sci Rep* 7(1)**,** 16270. doi: 10.1038/s41598-017-16465-4.

Heng, B.C., Cao, T., Stanton, L.W., Robson, P., and Olsen, B. (2004). Strategies for directing the differentiation of stem cells into the osteogenic lineage in vitro. *J Bone Miner Res* 19(9)**,** 1379-1394. doi: 10.1359/JBMR.040714.

Ho, S.S., Keown, A.T., Addison, B., and Leach, J.K. (2017). Cell Migration and Bone Formation from Mesenchymal Stem Cell Spheroids in Alginate Hydrogels Are Regulated by Adhesive Ligand Density. *Biomacromolecules* 18(12)**,** 4331-4340. doi: 10.1021/acs.biomac.7b01366.

Hsu, S.H., and Huang, G.S. (2013). Substrate-dependent Wnt signaling in MSC differentiation within biomaterial-derived 3D spheroids. *Biomaterials* 34(20)**,** 4725-4738. doi: 10.1016/j.biomaterials.2013.03.031.

Huggins, C.B. (1931). THE FORMATION OF BONE UNDER THE INFLUENCE OF EPITHELIUM OF THE URINARY TRACT. *JAMA Surgery* 22(3)**,** 377-408. doi: 10.1001/archsurg.1931.01160030026002.

Ingber, D.E., and Folkman, J. (1989). How does extracellular matrix control capillary morphogenesis? *Cell* 58(5)**,** 803-805.

Itoh, F., Asao, H., Sugamura, K., Heldin, C.H., ten Dijke, P., and Itoh, S. (2001). Promoting bone morphogenetic protein signaling through negative regulation of inhibitory Smads. *EMBO J* 20(15)**,** 4132-4142. doi: 10.1093/emboj/20.15.4132.

Javed, A., Chen, H., and Ghori, F.Y. (2010). Genetic and transcriptional control of bone formation. *Oral Maxillofac Surg Clin North Am* 22(3)**,** 283-293, v. doi: 10.1016/j.coms.2010.05.001.

Joyce, M.E., Roberts, A.B., Sporn, M.B., and Bolander, M.E. (1990). Transforming growth factor-beta and the initiation of chondrogenesis and osteogenesis in the rat femur. *J Cell Biol* 110(6)**,** 2195-2207.

Kakar, A., Rao, B.H.S., Hegde, S., Deshpande, N., Lindner, A., Nagursky, H., et al. (2017). Ridge preservation using an in situ hardening biphasic calcium phosphate (beta-TCP/HA) bone graft substitute-a clinical, radiological, and histological study. *Int J Implant Dent* 3(1)**,** 25. doi: 10.1186/s40729-017-0086-2.

Karageorgiou, V., and Kaplan, D. (2005). Porosity of 3D biomaterial scaffolds and osteogenesis. *Biomaterials* 26(27)**,** 5474-5491. doi: 10.1016/j.biomaterials.2005.02.002.

Reference

Katagiri, T., Osawa, K., Tsukamoto, S., Fujimoto, M., Miyamoto, A., and Mizuta, T. (2015). Bone morphogenetic protein-induced heterotopic bone formation: What have we learned from the history of a half century? *Japanese Dental Science Review* 51(2), 42-50. doi: https://doi.org/10.1016/j.jdsr.2014.09.004.

Katagiri, W., Sakaguchi, K., Kawai, T., Wakayama, Y., Osugi, M., and Hibi, H. (2017). A defined mix of cytokines mimics conditioned medium from cultures of bone marrow-derived mesenchymal stem cells and elicits bone regeneration. *Cell Prolif* 50(3). doi: 10.1111/cpr.12333.

Keating, J.F., and McQueen, M.M. (2001). Substitutes for autologous bone graft in orthopaedic trauma. *J Bone Joint Surg Br* 83(1), 3-8.

Kim, H., Suh, H., Jo, S.A., Kim, H.W., Lee, J.M., Kim, E.H., et al. (2005). In vivo bone formation by human marrow stromal cells in biodegradable scaffolds that release dexamethasone and ascorbate-2-phosphate. *Biochem Biophys Res Commun* 332(4), 1053-1060. doi: 10.1016/j.bbrc.2005.05.051.

Kim, J., and Ma, T. (2012). Perfusion regulation of hMSC microenvironment and osteogenic differentiation in 3D scaffold. *Biotechnol Bioeng* 109(1), 252-261. doi: 10.1002/bit.23290.

Kishimoto, Y., Saito, N., Kurita, K., Shimokado, K., Maruyama, N., and Ishigami, A. (2013). Ascorbic acid enhances the expression of type 1 and type 4 collagen and SVCT2 in cultured human skin fibroblasts. *Biochem Biophys Res Commun* 430(2), 579-584. doi: 10.1016/j.bbrc.2012.11.110.

Klar, R.M. (2018). The Induction of Bone Formation: The Translation Enigma. *Front Bioeng Biotechnol* 6, 74. doi: 10.3389/fbioe.2018.00074.

Klar, R.M., Duarte, R., Dix-Peek, T., Dickens, C., Ferretti, C., and Ripamonti, U. (2013). Calcium ions and osteoclastogenesis initiate the induction of bone formation by coral-derived macroporous constructs. *J Cell Mol Med* 17(11), 1444-1457. doi: 10.1111/jcmm.12125.

Klar, R.M., Duarte, R., Dix-Peek, T., and Ripamonti, U. (2014). The induction of bone formation by the recombinant human transforming growth factor-beta3. *Biomaterials* 35(9), 2773-2788. doi: 10.1016/j.biomaterials.2013.12.062.

Kneser, U., Polykandriotis, E., Ohnolz, J., Heidner, K., Grabinger, L., Euler, S., et al. (2006). Engineering of vascularized transplantable bone tissues: induction of axial vascularization in an osteoconductive matrix using an arteriovenous loop. *Tissue Eng* 12(7), 1721-1731. doi: 10.1089/ten.2006.12.1721.

Komori, T. (2017). Roles of Runx2 in Skeletal Development. *Adv Exp Med Biol* 962, 83-93. doi: 10.1007/978-981-10-3233-2_6.

Kon, E., Muraglia, A., Corsi, A., Bianco, P., Marcacci, M., Martin, I., et al. (2000). Autologous bone marrow stromal cells loaded onto porous hydroxyapatite ceramic accelerate bone repair in critical-size defects of sheep long bones. *J Biomed Mater Res* 49(3), 328-337.

Kubo, S., Cooper, G.M., Matsumoto, T., Phillippi, J.A., Corsi, K.A., Usas, A., et al. (2009). Blocking vascular endothelial growth factor with soluble Flt-1 improves the chondrogenic potential of mouse skeletal muscle-derived stem cells. *Arthritis Rheum* 60(1), 155-165. doi: 10.1002/art.24153.

Lacroix, P. (1945). Recent investigations on the growth of bone. *Nature* 156(3967), 576.

Ladd, A.L., and Pliam, N.B. (1999). Use of bone-graft substitutes in distal radius fractures. *J Am Acad Orthop Surg* 7(5), 279-290.

Langenbach, F., and Handschel, J. (2013). Effects of dexamethasone, ascorbic acid and beta-glycerophosphate on the osteogenic differentiation of stem cells in vitro. *Stem Cell Res Ther* 4(5), 117. doi: 10.1186/scrt328.

Lefebvre, V. (2019). Roles and regulation of SOX transcription factors in skeletogenesis. *Curr Top Dev Biol* 133, 171-193. doi: 10.1016/bs.ctdb.2019.01.007.

Reference

Leighton, J., Mark, R., and Justh, G. (1968). Patterns of three-dimensional growth in vitro in collagen-coated cellulose sponge: carcinomas and embryonic tissues. *Cancer Res* 28(2)**,** 286-296.

Lennon, D.P., Haynesworth, S.E., Young, R.G., Dennis, J.E., and Caplan, A.I. (1995). A chemically defined medium supports in vitro proliferation and maintains the osteochondral potential of rat marrow-derived mesenchymal stem cells. *Exp Cell Res* 219(1)**,** 211-222. doi: 10.1006/excr.1995.1221.

Levander, G. (1938). A study of bone regeneration. *Surg. Gynec. Obstet.* 67**,** 705-748.

Levander, G. (1945). Tissue Induction. *Nature* 155(3927)**,** 148-149. doi: 10.1038/155148a0.

Lewis, A., Lee, J.Y., Donaldson, A.V., Natanek, S.A., Vaidyanathan, S., Man, W.D., et al. (2016). Increased expression of H19/miR-675 is associated with a low fat-free mass index in patients with COPD. *J Cachexia Sarcopenia Muscle* 7(3)**,** 330-344. doi: 10.1002/jcsm.12078.

Lin, L., Fu, X., Zhang, X., Chen, L.X., Zhang, J.Y., Yu, C.L., et al. (2006). Rat adipose-derived stromal cells expressing BMP4 induce ectopic bone formation in vitro and in vivo. *Acta Pharmacol Sin* 27(12)**,** 1608-1615. doi: 10.1111/j.1745-7254.2006.00449.x.

Lin, L., Shen, Q., Xue, T., and Yu, C. (2010). Heterotopic ossification induced by Achilles tenotomy via endochondral bone formation: expression of bone and cartilage related genes. *Bone* 46(2)**,** 425-431. doi: 10.1016/j.bone.2009.08.057.

Linovitz, R.J., and Peppers, T.A. (2002). Use of an advanced formulation of beta-tricalcium phosphate as a bone extender in interbody lumbar fusion. *Orthopedics* 25(5 Suppl)**,** s585-589.

Liu, Y., Teoh, S.H., Chong, M.S., Yeow, C.H., Kamm, R.D., Choolani, M., et al. (2013). Contrasting effects of vasculogenic induction upon biaxial bioreactor stimulation of mesenchymal stem cells and endothelial progenitor cells cocultures in three-dimensional scaffolds under in vitro and in vivo paradigms for vascularized bone tissue engineering. *Tissue Eng Part A* 19(7-8)**,** 893-904. doi: 10.1089/ten.TEA.2012.0187.

Livingston, T., Ducheyne, P., and Garino, J. (2002). In vivo evaluation of a bioactive scaffold for bone tissue engineering. *J Biomed Mater Res* 62(1)**,** 1-13. doi: 10.1002/jbm.10157.

Livingston, T.L., Gordon, S., Archambault, M., Kadiyala, S., McIntosh, K., Smith, A., et al. (2003). Mesenchymal stem cells combined with biphasic calcium phosphate ceramics promote bone regeneration. *J Mater Sci Mater Med* 14(3)**,** 211-218.

Lu, J.X., Flautre, B., Anselme, K., Hardouin, P., Gallur, A., Descamps, M., et al. (1999). Role of interconnections in porous bioceramics on bone recolonization in vitro and in vivo. *J Mater Sci Mater Med* 10(2)**,** 111-120.

Lu, J.X., Gallur, A., Flautre, B., Anselme, K., Descamps, M., Thierry, B., et al. (1998). Comparative study of tissue reactions to calcium phosphate ceramics among cancellous, cortical, and medullar bone sites in rabbits. *J Biomed Mater Res* 42(3)**,** 357-367.

Luedi, M.M., Singh, S.K., Mosley, J.C., Hassan, I.S.A., Hatami, M., Gumin, J., et al. (2018). Dexamethasone-mediated oncogenicity in vitro and in an animal model of glioblastoma. *J Neurosurg* 129(6)**,** 1446-1455. doi: 10.3171/2017.7.JNS17668.

Martin, I., Wendt, D., and Heberer, M. (2004). The role of bioreactors in tissue engineering. *Trends Biotechnol* 22(2)**,** 80-86. doi: 10.1016/j.tibtech.2003.12.001.

Martinez-Sanchez, A., Dudek, K.A., and Murphy, C.L. (2012). Regulation of human chondrocyte function through direct inhibition of cartilage master regulator SOX9 by microRNA-145 (miRNA-145). *J Biol Chem* 287(2)**,** 916-924. doi: 10.1074/jbc.M111.302430.

Mastrogiacomo, M., Scaglione, S., Martinetti, R., Dolcini, L., Beltrame, F., Cancedda, R., et al. (2006). Role of scaffold internal structure on in vivo bone formation in macroporous calcium phosphate bioceramics. *Biomaterials* 27(17)**,** 3230-3237. doi: 10.1016/j.biomaterials.2006.01.031.

Mauney, J.R., Blumberg, J., Pirun, M., Volloch, V., Vunjak-Novakovic, G., and Kaplan, D.L. (2004). Osteogenic differentiation of human bone marrow stromal cells on partially demineralized bone scaffolds in vitro. *Tissue Eng* 10(1-2)**,** 81-92. doi: 10.1089/107632704322791727.

Reference

Mauney, J.R., Jaquiery, C., Volloch, V., Heberer, M., Martin, I., and Kaplan, D.L. (2005). In vitro and in vivo evaluation of differentially demineralized cancellous bone scaffolds combined with human bone marrow stromal cells for tissue engineering. *Biomaterials* 26(16)**,** 3173-3185. doi: 10.1016/j.biomaterials.2004.08.020.

Mayer, H., Bertram, H., Lindenmaier, W., Korff, T., Weber, H., and Weich, H. (2005). Vascular endothelial growth factor (VEGF-A) expression in human mesenchymal stem cells: autocrine and paracrine role on osteoblastic and endothelial differentiation. *J Cell Biochem* 95(4)**,** 827-839. doi: 10.1002/jcb.20462.

McCluskey, J., and Gutteridge, D.H. (1982). Avascular necrosis of bone after high doses of dexamethasone during neurosurgery. *Br Med J (Clin Res Ed)* 284(6312)**,** 333-334. doi: 10.1136/bmj.284.6312.333.

McKee, C., and Chaudhry, G.R. (2017). Advances and challenges in stem cell culture. *Colloids Surf B Biointerfaces* 159**,** 62-77. doi: 10.1016/j.colsurfb.2017.07.051.

Meinel, L., Karageorgiou, V., Hofmann, S., Fajardo, R., Snyder, B., Li, C., et al. (2004). Engineering bone-like tissue in vitro using human bone marrow stem cells and silk scaffolds. *J Biomed Mater Res A* 71(1)**,** 25-34. doi: 10.1002/jbm.a.30117.

Mendez-Ferrer, S., Michurina, T.V., Ferraro, F., Mazloom, A.R., Macarthur, B.D., Lira, S.A., et al. (2010). Mesenchymal and haematopoietic stem cells form a unique bone marrow niche. *Nature* 466(7308)**,** 829-834. doi: 10.1038/nature09262.

Mitra, D., Whitehead, J., Yasui, O.W., and Leach, J.K. (2017). Bioreactor culture duration of engineered constructs influences bone formation by mesenchymal stem cells. *Biomaterials* 146**,** 29-39. doi: 10.1016/j.biomaterials.2017.08.044.

Moreira-Gonzalez, A., Lobocki, C., Barakat, K., Andrus, L., Bradford, M., Gilsdorf, M., et al. (2005). Evaluation of 45S5 bioactive glass combined as a bone substitute in the reconstruction of critical size calvarial defects in rabbits. *J Craniofac Surg* 16(1)**,** 63-70.

Morgoulis, D., Berenstein, P., Cazacu, S., Kazimirsky, G., Dori, A., Barnea, E.R., et al. (2019). sPIF promotes myoblast differentiation and utrophin expression while inhibiting fibrosis in Duchenne muscular dystrophy via the H19/miR-675/let-7 and miR-21 pathways. *Cell Death Dis* 10(2)**,** 82. doi: 10.1038/s41419-019-1307-9.

Movat, H.Z. (1955). Demonstration of all connective tissue elements in a single section; pentachrome stains. *AMA Arch Pathol* 60(3)**,** 289-295.

Mussano, F., Ciccone, G., Ceccarelli, M., Baldi, I., and Bassi, F. (2007). Bone morphogenetic proteins and bone defects: a systematic review. *Spine (Phila Pa 1976)* 32(7)**,** 824-830. doi: 10.1097/01.brs.0000259227.51180.ca.

Nakagawa, H., Takagi, K., Kitaoka, M., Iyama, K.I., and Usuku, G. (1993). Influence of monocyte-macrophage lineage cells on alkaline phosphatase activity of developing osteoblasts derived from rat bone marrow stromal cells. *Nihon Seikeigeka Gakkai Zasshi* 67(5)**,** 480-489.

Nazarov, R., Jin, H.J., and Kaplan, D.L. (2004). Porous 3-D scaffolds from regenerated silk fibroin. *Biomacromolecules* 5(3)**,** 718-726. doi: 10.1021/bm034327e.

Nelson, D.L., and Cox, M. (2005). *Lehninger principles of biochemistry (4th ed.).* New York: W.H. Freeman and Company.

Nguyen, B.N., Ko, H., and Fisher, J.P. (2016). Tunable osteogenic differentiation of hMPCs in tubular perfusion system bioreactor. *Biotechnol Bioeng* 113(8)**,** 1805-1813. doi: 10.1002/bit.25929.

Nkenke, E., and Stelzle, F. (2009). Clinical outcomes of sinus floor augmentation for implant placement using autogenous bone or bone substitutes: a systematic review. *Clin Oral Implants Res* 20 Suppl 4**,** 124-133. doi: 10.1111/j.1600-0501.2009.01776.x.

Ollier, L. (1867). *Traité expérimental et clinique de la régénération des os et de la production artificielle du tissu osseux.* V. Masson.

Reference

Pang, E.K., Im, S.U., Kim, C.S., Choi, S.H., Chai, J.K., Kim, C.K., et al. (2004). Effect of recombinant human bone morphogenetic protein-4 dose on bone formation in a rat calvarial defect model. *J Periodontol* 75(10)**,** 1364-1370. doi: 10.1902/jop.2004.75.10.1364.

Plunkett, N., and O'Brien, F.J. (2011). Bioreactors in tissue engineering. *Technol Health Care* 19(1)**,** 55-69. doi: 10.3233/THC-2011-0605.

Polykandriotis, E., Arkudas, A., Beier, J.P., Hess, A., Greil, P., Papadopoulos, T., et al. (2007). Intrinsic axial vascularization of an osteoconductive bone matrix by means of an arteriovenous vascular bundle. *Plast Reconstr Surg* 120(4)**,** 855-868. doi: 10.1097/01.prs.0000277664.89467.14.

Reddi, A.H. (1994). Symbiosis of biotechnology and biomaterials: applications in tissue engineering of bone and cartilage. *J Cell Biochem* 56(2)**,** 192-195. doi: 10.1002/jcb.240560213.

Reddi, A.H. (1998). Role of morphogenetic proteins in skeletal tissue engineering and regeneration. *Nat Biotechnol* 16(3)**,** 247-252. doi: 10.1038/nbt0398-247.

Reddi, A.H. (2000). Morphogenesis and tissue engineering of bone and cartilage: inductive signals, stem cells, and biomimetic biomaterials. *Tissue Eng* 6(4)**,** 351-359. doi: 10.1089/107632700418074.

Reddi, A.H., and Huggins, C. (1972). Biochemical sequences in the transformation of normal fibroblasts in adolescent rats. *Proceedings of the National Academy of Sciences of the United States of America* 69(6)**,** 1601-1605. doi: 10.1073/pnas.69.6.1601.

Reichert, J.C., Saifzadeh, S., Wullschleger, M.E., Epari, D.R., Schutz, M.A., Duda, G.N., et al. (2009). The challenge of establishing preclinical models for segmental bone defect research. *Biomaterials* 30(12)**,** 2149-2163. doi: 10.1016/j.biomaterials.2008.12.050.

Riley, E.H., Lane, J.M., Urist, M.R., Lyons, K.M., and Lieberman, J.R. (1996). Bone morphogenetic protein-2: biology and applications. *Clin Orthop Relat Res* (324)**,** 39-46.

Ripamonti, U. (1990). *Handbook of Bioactive Ceramics: Volume II Calcium Phosphate and Hydroxyapatite Ceramics): Inductive bone matrix and porous hydroxyapatite composites in rodents and non-human primates.* Boca Raton: FL: CRC Press.

Ripamonti, U. (1991). The morphogenesis of bone in replicas of porous hydroxyapatite obtained from conversion of calcium carbonate exoskeletons of coral. *J Bone Joint Surg Am* 73(5)**,** 692-703.

Ripamonti, U. (2006). Soluble osteogenic molecular signals and the induction of bone formation. *Biomaterials* 27(6)**,** 807-822. doi: 10.1016/j.biomaterials.2005.09.021.

Ripamonti, U., Heliotis, M., and Ferretti, C. (2007). Bone morphogenetic proteins and the induction of bone formation: from laboratory to patients. *Oral Maxillofac Surg Clin North Am* 19(4)**,** 575-589, vii. doi: 10.1016/j.coms.2007.07.006.

Ripamonti, U., Klar, R.M., Parak, R., Dickens, C., Dix-Peek, T., and Duarte, R. (2016). Tissue segregation restores the induction of bone formation by the mammalian transforming growth factor-beta(3) in calvarial defects of the non-human primate Papio ursinus. *Biomaterials* 86**,** 21-32. doi: 10.1016/j.biomaterials.2016.01.071.

Ripamonti, U., Klar, R.M., Renton, L.F., and Ferretti, C. (2010). Synergistic induction of bone formation by hOP-1, hTGF-beta3 and inhibition by zoledronate in macroporous coral-derived hydroxyapatites. *Biomaterials* 31(25)**,** 6400-6410. doi: 10.1016/j.biomaterials.2010.04.037.

Ripamonti, U., Petit, J.C., and Teare, J. (2009). Cementogenesis and the induction of periodontal tissue regeneration by the osteogenic proteins of the transforming growth factor-beta superfamily. *J Periodontal Res* 44(2)**,** 141-152. doi: 10.1111/j.1600-0765.2008.01158.x.

Risau, W. (1997). Mechanisms of angiogenesis. *Nature* 386(6626)**,** 671-674. doi: 10.1038/386671a0.

Roach, H.I. (1990). Long-term organ culture of embryonic chick femora: a system for investigating bone and cartilage formation at an intermediate level of organization. *J Bone Miner Res* 5(1)**,** 85-100. doi: 10.1002/jbmr.5650050113.

Rosen, D., Miller, S.C., DeLeon, E., Thompson, A.Y., Bentz, H., Mathews, M., et al. (1994). Systemic administration of recombinant transforming growth factor beta 2 (rTGF-beta 2)

stimulates parameters of cancellous bone formation in juvenile and adult rats. *Bone* 15(3)**,** 355-359.

Sakakura, Y., Fujiwara, N., and Nawa, T. (1989). A simple, disposable, and improved organ culture system for maintaining three-dimensional development of mouse embryonic molars. *In Vitro Cell Dev Biol* 25(10)**,** 959-964.

Sampath, T.K., and Reddi, A.H. (1981). Dissociative extraction and reconstitution of extracellular matrix components involved in local bone differentiation. *Proc Natl Acad Sci U S A* 78(12)**,** 7599-7603.

Schipani, E., Mangiavini, L., and Merceron, C. (2013). ATF4 and HIF-1alpha in bone: an intriguing relationship. *J Bone Miner Res* 28(9)**,** 1866-1869. doi: 10.1002/jbmr.2045.

Senn, N. (1889). On the Healing of Aseptic Bone Cavities by Implantation of Antiseptic Decalcified Bone. *Am J Med Sci* 98**,** 219ß243.

Sharma, D., Ross, D., Wang, G., Jia, W., Kirkpatrick, S.J., and Zhao, F. (2019). Upgrading prevascularization in tissue engineering: A review of strategies for promoting highly organized microvascular network formation. *Acta Biomater*. doi: 10.1016/j.actbio.2019.03.016.

Shors, E.C. (1999). Coralline bone graft substitutes. *Orthop Clin North Am* 30(4)**,** 599-613.

Simic, P., Culej, J.B., Orlic, I., Grgurevic, L., Draca, N., Spaventi, R., et al. (2006). Systemically administered bone morphogenetic protein-6 restores bone in aged ovariectomized rats by increasing bone formation and suppressing bone resorption. *J Biol Chem* 281(35)**,** 25509-25521. doi: 10.1074/jbc.M513276200.

Sinha, A., and Vyavahare, N.R. (2013). High-glucose levels and elastin degradation products accelerate osteogenesis in vascular smooth muscle cells. *Diab Vasc Dis Res* 10(5)**,** 410-419. doi: 10.1177/1479164113485101.

Sorice, A., Guerriero, E., Capone, F., Colonna, G., Castello, G., and Costantini, S. (2014). Ascorbic acid: its role in immune system and chronic inflammation diseases. *Mini Rev Med Chem* 14(5)**,** 444-452.

Sottile, V., Thomson, A., and McWhir, J. (2003). In vitro osteogenic differentiation of human ES cells. *Cloning Stem Cells* 5(2)**,** 149-155. doi: 10.1089/153623003322234759.

Steck, E., Boeuf, S., Gabler, J., Werth, N., Schnatzer, P., Diederichs, S., et al. (2012). Regulation of H19 and its encoded microRNA-675 in osteoarthritis and under anabolic and catabolic in vitro conditions. *J Mol Med (Berl)* 90(10)**,** 1185-1195. doi: 10.1007/s00109-012-0895-y.

Sul, Y.T., Johansson, C., Byon, E., and Albrektsson, T. (2005). The bone response of oxidized bioactive and non-bioactive titanium implants. *Biomaterials* 26(33)**,** 6720-6730. doi: 10.1016/j.biomaterials.2005.04.058.

Trueta, J. (1963). The role of the vessels in osteogenesis. *Bone Joint Surg* 45 B**,** 402-418.

Trzeciak, T., and Czarny-Ratajczak, M. (2014). MicroRNAs: Important Epigenetic Regulators in Osteoarthritis. *Curr Genomics* 15(6)**,** 481-484. doi: 10.2174/1389202915666141024212506.

Tsimbouri, P.M., Childs, P.G., Pemberton, G.D., Yang, J., Jayawarna, V., Orapiriyakul, W., et al. (2017). Stimulation of 3D osteogenesis by mesenchymal stem cells using a nanovibrational bioreactor. *Nat Biomed Eng* 1(9)**,** 758-770. doi: 10.1038/s41551-017-0127-4.

Urist, M.R. (1965). Bone: formation by autoinduction. *Science* 150(3698)**,** 893-899.

Urist, M.R., Silverman, B.F., Buring, K., Dubuc, F.L., and Rosenberg, J.M. (1967). The bone induction principle. *Clin Orthop Relat Res* 53**,** 243-283.

Urist, M.R., and Strates, B.S. (1971). Bone Morphogenetic Protein. *Journal of Dental Research* 50(6)**,** 1392-1406. doi: 10.1177/00220345710500060601.

Vailhé, B., Vittet, D., and Feige, J.-J. (2001). In Vitro Models of Vasculogenesis and Angiogenesis. *Laboratory Investigation* 81**,** 439. doi: 10.1038/labinvest.3780252.

Vernon, R.B., Lara, S.L., Drake, C.J., Iruela-Arispe, M.L., Angello, J.C., Little, C.D., et al. (1995). Organized type I collagen influences endothelial patterns during "spontaneous angiogenesis in vitro": planar cultures as models of vascular development. *In Vitro Cell Dev Biol Anim* 31(2)**,** 120-131. doi: 10.1007/BF02633972.

Vittet, D., Buchou, T., Schweitzer, A., Dejana, E., and Huber, P. (1997). Targeted null-mutation in the vascular endothelial-cadherin gene impairs the organization of vascular-like structures in embryoid bodies. *Proc Natl Acad Sci U S A* 94(12)**,** 6273-6278.

Vrselja, Z., Daniele, S.G., Silbereis, J., Talpo, F., Morozov, Y.M., Sousa, A.M.M., et al. (2019). Restoration of brain circulation and cellular functions hours post-mortem. *Nature* 568(7752)**,** 336-343. doi: 10.1038/s41586-019-1099-1.

Wang, E.A., Rosen, V., Cordes, P., Hewick, R.M., Kriz, M.J., Luxenberg, D.P., et al. (1988). Purification and characterization of other distinct bone-inducing factors. *Proc Natl Acad Sci U S A* 85(24)**,** 9484-9488. doi: 10.1073/pnas.85.24.9484.

Wang, E.A., Rosen, V., D'Alessandro, J.S., Bauduy, M., Cordes, P., Harada, T., et al. (1990). Recombinant human bone morphogenetic protein induces bone formation. *Proc Natl Acad Sci U S A* 87(6)**,** 2220-2224. doi: 10.1073/pnas.87.6.2220.

Wang, L., Zhang, B., Bao, C., Habibovic, P., Hu, J., and Zhang, X. (2014). Ectopic osteoid and bone formation by three calcium-phosphate ceramics in rats, rabbits and dogs. *PLoS One* 9(9)**,** e107044. doi: 10.1371/journal.pone.0107044.

Wartenberg, M., Gunther, J., Hescheler, J., and Sauer, H. (1998). The embryoid body as a novel in vitro assay system for antiangiogenic agents. *Lab Invest* 78(10)**,** 1301-1314.

White, E.W., Weber, J.N., Roy, D.M., Owen, E.L., Chiroff, R.T., and White, R.A. (1975). Replamineform porous biomaterials for hard tissue implant applications. *J Biomed Mater Res* 9(4)**,** 23-27. doi: 10.1002/jbm.820090406.

Willestaedt, H., Levander, G., and Hult, L. (1950). Studies in osteogenesis. *Acta Orthopaedica Scandinavica* 19(4)**,** 419-432.

Wozney, J.M., Rosen, V., Celeste, A.J., Mitsock, L.M., Whitters, M.J., Kriz, R.W., et al. (1988). Novel regulators of bone formation: molecular clones and activities. *Science* 242(4885)**,** 1528-1534. doi: 10.1126/science.3201241.

Xu, R., Khan, S.K., Zhou, T., Gao, B., Zhou, Y., Zhou, X., et al. (2018). Gαs signaling controls intramembranous ossification during cranial bone development by regulating both Hedgehog and Wnt/β-catenin signaling. *Bone Research* 6(1)**,** 33. doi: 10.1038/s41413-018-0034-7.

Yablonka-Reuveni, Z. (2011). The skeletal muscle satellite cell: still young and fascinating at 50. *J Histochem Cytochem* 59(12)**,** 1041-1059. doi: 10.1369/0022155411426780.

Yang, J., Andre, P., Ye, L., and Yang, Y.Z. (2015). The Hedgehog signalling pathway in bone formation. *Int J Oral Sci* 7(2)**,** 73-79. doi: 10.1038/ijos.2015.14.

Yang, J., Zhang, Y.S., Yue, K., and Khademhosseini, A. (2017). Cell-laden hydrogels for osteochondral and cartilage tissue engineering. *Acta Biomater* 57**,** 1-25. doi: 10.1016/j.actbio.2017.01.036.

Ye, K., Traianedes, K., Choong, P.F., and Myers, D.E. (2016). Chondrogenesis of Human Infrapatellar Fat Pad Stem Cells on Acellular Dermal Matrix. *Front Surg* 3**,** 3. doi: 10.3389/fsurg.2016.00003.

Yuen, H.F., Kwok, W.K., Chan, K.K., Chua, C.W., Chan, Y.P., Chu, Y.Y., et al. (2008). TWIST modulates prostate cancer cell-mediated bone cell activity and is upregulated by osteogenic induction. *Carcinogenesis* 29(8)**,** 1509-1518. doi: 10.1093/carcin/bgn105.

Zhu, W.H., Guo, X., Villaschi, S., and Francesco Nicosia, R. (2000). Regulation of vascular growth and regression by matrix metalloproteinases in the rat aorta model of angiogenesis. *Lab Invest* 80(4)**,** 545-555.

zur Nieden, N.I., Kempka, G., and Ahr, H.J. (2003). In vitro differentiation of embryonic stem cells into mineralized osteoblasts. *Differentiation* 71(1)**,** 18-27. doi: 10.1046/j.1432-0436.2003.700602.x.